

# Dietary nucleic acids promote oral tolerance through innate sensing pathways in mice

Received: 26 February 2024

Accepted: 23 October 2024

Published online: 01 November 2024



Tao Yang<sup>1</sup>, Tian Li<sup>1</sup>, Yingying Xing<sup>1</sup>, Mengtao Cao<sup>1</sup>, Mingxiang Zhang<sup>2</sup>, Qibin Leng<sup>3</sup>, Ju Qiu<sup>1</sup>, Xinyang Song<sup>4</sup>, Jianfeng Chen<sup>4</sup>, Guohong Hu<sup>1</sup> & Youcun Qian<sup>1,2</sup>✉

Oral tolerance is essential for intestinal homeostasis and systemic immune function. However, our understanding of how oral tolerance is maintained is inadequate. Here we report that food-derived nucleic acids promote oral tolerance through innate sensing pathways. We find that dietary nucleic acids, but not microbiota, expand the natural intraepithelial lymphocyte (IEL) pool, specifically in the small intestine. TGF- $\beta$ 1, produced by natural IELs, then promotes activation of gut CD103<sup>+</sup> dendritic cells to support the induction of antigen-specific Treg cells in a mouse model of OVA-induced oral tolerance. Mechanistically, MAVS and STING are redundantly required for sensing dietary RNAs and DNAs to activate downstream TBK1 signalling to induce IL-15 production, which results in the accumulation of natural IELs. Thus, our study demonstrates a key role of food-triggered innate sensing pathways in the maintenance of natural IELs and oral tolerance.

As the main organ responsible for absorbing nutrients from food, the intestine is regularly exposed to significant quantities of foreign antigenic substances<sup>1</sup>. In order to preserve its homeostasis and function, the intestine must, therefore, develop a sophisticated mucosal immune system to deal with these external antigens<sup>2,3</sup>. To effectively manage these challenges, the body actively induces and establishes oral tolerance, which suppresses both local and systemic immune reactions to substances that have been ingested orally<sup>4,5</sup>. Over the past few decades, research on oral tolerance has shown that a variety of cellular and molecular processes are involved in this process<sup>5–7</sup>. However, we still do not fully understand how oral tolerance is established and maintained.

Within the intestinal epithelium, intraepithelial lymphocytes (IEL) are the predominant local immune cells and are in close contact with a variety of luminal antigens<sup>8</sup>. The majority of IELs are TCR $\alpha$ <sup>+</sup> T cells and can be divided into two groups: the induced (or adaptive) IELs and the natural IELs. The induced IELs are mainly composed of the TCR $\alpha$  $\beta$ <sup>+</sup>CD4<sup>+</sup> and TCR $\alpha$  $\beta$ <sup>+</sup>CD8 $\alpha$  $\beta$ <sup>+</sup> subsets<sup>9</sup>. These cells are

conventional resident memory T cells that are first selected in the thymus and then enter the intestinal epithelium by acquiring IEL markers for local residency<sup>10</sup>. The natural IELs contain TCR $\alpha$  $\beta$ <sup>+</sup>CD8 $\alpha$  $\alpha$ <sup>+</sup> and TCR $\gamma$  $\delta$ <sup>+</sup> subsets. These IEL subsets are unique to the intestine, as they are not observed in the conventional peripheral lymphoid organs<sup>11</sup>. While TCR $\gamma$  $\delta$ <sup>+</sup> natural IELs develop mainly extrathymically, TCR $\alpha$  $\beta$ <sup>+</sup>CD8 $\alpha$  $\alpha$ <sup>+</sup> natural IELs are selected in the thymus<sup>12</sup>. The CD4<sup>+</sup>CD8<sup>+</sup>TCR $\alpha$  $\beta$ <sup>+</sup> precursors migrate from the thymus into the intestinal epithelium, where they receive local signals to complete their development into TCR $\alpha$  $\beta$ <sup>+</sup>CD8 $\alpha$  $\alpha$ <sup>+</sup> natural IELs<sup>13</sup>. The critical cytokine signals from the intestine, such as IL-15, TGF- $\beta$ , and IL-7, are essential for the development and maintenance of natural IELs<sup>14</sup>. What is yet unknown, though, are the original factors that cause the local cytokine production.

The interrelationship between the intestinal immune system and the microbiota is critical for gut homeostasis<sup>15</sup>. Although microbiota is required for the development and maintenance of the induced IELs, it is dispensable for the development and maintenance of the

<sup>1</sup>CAS Key Laboratory of Tissue Microenvironment and Tumor, Shanghai Institute of Nutrition and Health, University of Chinese Academy of Sciences, Chinese Academy of Sciences, Shanghai 200031, China. <sup>2</sup>School of Life Science and Technology, ShanghaiTech University, Shanghai 200031, China. <sup>3</sup>Affiliated Cancer Hospital & Institute of Guangzhou Medical University, State Key Laboratory of Respiratory Disease, Guangzhou 510180, China. <sup>4</sup>State Key Laboratory of Cell Biology, CAS Center for Excellence in Molecular Cell Science, Shanghai Institute of Biochemistry and Cell Biology, Chinese Academy of Sciences, University of Chinese Academy of Sciences, Shanghai 200031, China. ✉e-mail: [ycqian@sinh.ac.cn](mailto:ycqian@sinh.ac.cn)

natural IELs<sup>16–18</sup>. Notably, while microbiota predominantly populates in the large intestine, the majority of natural IELs reside in the small intestine rather than the colon<sup>19,20</sup>, suggesting that the development of natural IELs requires specialized local niche support from the small intestine.

In this study, we conduct a comprehensive investigation into the effects of innate sensor pathway deficiencies on the development of natural IELs in mice under normal physiological conditions. We find that dietary nucleic acids, through specific innate sensing mechanisms, provided the necessary signals for the persistence and functionality of natural IELs, independent of microbial influences. We further demonstrate that these natural IELs are integral to the establishment of oral tolerance, a process by which the immune system becomes unresponsive or tolerant to harmless antigens encountered through the diet. Thus, our findings highlight the fundamental role of natural IELs in the well-developed mucosal immune network and emphasize the importance of innate sensing mechanisms in regulating immune responses to dietary antigens.

## Results

### MAVS and STING are redundantly required for the development of natural IELs

It is still unclear how natural IELs are maintained in the intestine. We wondered whether innate sensing pathways are involved in modulating natural IELs. Considering the cascading redundancy of innate sensing receptors, we investigated the potential roles of major downstream adaptors such as MyD88, TRIF, MAVS, and STING in IEL development. Consistent with a previous report<sup>21</sup>, *Myd88*-deficient mice showed less than twofold reduction of the TCR $\gamma\delta^+$  and TCR $\alpha\beta^+$ CD8 $\alpha\alpha^+$  IELs in the small intestine (Supplementary Fig. 1a–d), while the percentage or number of the induced IELs did not change (Supplementary Fig. 1c–e). In parallel to MyD88, deficiency of TRIF, MAVS, or STING alone in mice did not affect the percentages or numbers of either natural IELs or induced IELs (Fig. 1a–c). However, we found that double deficiency of MAVS and STING (MS DKO) in mice dramatically reduced the percentages and numbers of TCR $\gamma\delta^+$  and TCR $\alpha\beta^+$ CD8 $\alpha\alpha^+$  natural IELs in the small intestine (Fig. 1a–c and

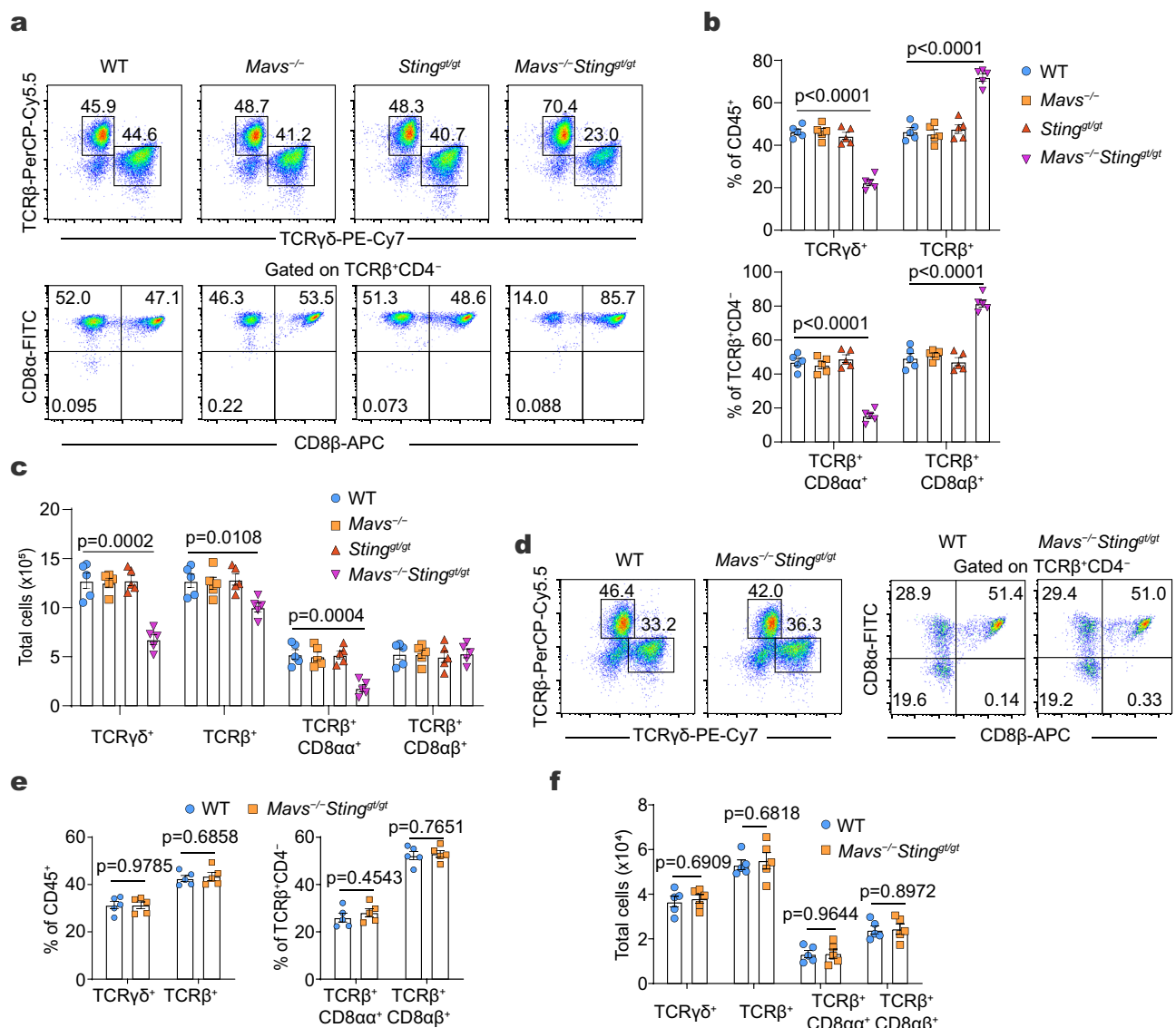


**Fig. 1 | MAVS and STING signaling pathways are redundantly required for the development of natural IELs in the small intestine.** **a–c** Representative flow plots (**a**), cell percentages (**b**), and cell numbers (**c**) of small intestinal IELs from WT, *Mavs* $^{-/-}$ , *Sting* $^{gt/lt}$ , or *Mavs* $^{-/-}$ *Sting* $^{gt/lt}$  mice,  $n = 5$ . **d–f** Representative flow plots (**d**), cell percentages (**e**), and cell numbers (**f**) of colon IELs from WT or *Mavs* $^{-/-}$ *Sting* $^{gt/lt}$

mice,  $n = 5$ . Data are mean  $\pm$  s.e.m. and from one experiment representative of three independent experiments. Statistics: one-way ANOVA followed by the Bonferroni post hoc test (**b, c**) or two-tailed, Student's *t* tests (**e, f**). Source data are provided as a Source Data file.

Supplementary Fig. 1f). Due to the percentage reduction of the natural IELs, the percentage of the induced  $\text{TCR}\alpha\beta^+\text{CD8}\alpha\beta^+$  IELs was increased, while the number of these induced IELs remained intact in the double-deficient mice (Fig. 1a–c). Additionally, the double loss of MAVS and STING did not influence the development of  $\text{CD4}^+$  and  $\text{CD8}^+$  T cells in the thymus, spleen, mesenteric lymph nodes, Peyer's patches, and small intestinal lamina propria (LP, Supplementary Fig. 1g–i). Furthermore, the frequencies of basal Treg cells in the small intestine or Tfh and B cells in the germinal center in MS DKO mice remained unaltered (Supplementary Fig. 1j). Taken together, these data indicate that MAVS-mediated RNA sensing and STING-mediated DNA sensing pathways are redundant and essential for the development of intestinal natural IELs. Although natural IELs appear largely in the small intestine and in limited quantities in the colon<sup>19</sup>, we also examined the colons of MS DKO mice and found no changes in natural IELs (Fig. 1d–f). Thus, our findings indicate that unique microenvironmental cues within the small intestine activate the innate sensing pathways to regulate the natural IEL pool.

### Dietary nucleic acids promote the development of natural IELs in the small intestine

Although an early study claimed that the gut microbiota contributes to the accumulation of intestinal natural IELs<sup>22</sup>, the other studies in germ-free (GF) mice demonstrated that the development and maintenance of natural IELs are independent of the microbiota<sup>16–18</sup>. We also found that the percentages and total numbers of the induced IELs, e.g.,  $\text{TCR}\beta^+\text{CD8}\alpha\beta^+$ ,  $\text{TCR}\beta^+\text{CD4}^+$ , and  $\text{TCR}\beta^+\text{CD4}^+\text{CD8}\alpha\alpha^+$  cells, were significantly reduced in the small intestine of GF mice compared to that of specific pathogen-free (SPF) mice, whereas the numbers of the natural  $\text{TCR}\gamma\delta^+$  and  $\text{TCR}\alpha\beta^+\text{CD8}\alpha\alpha^+$  IELs were not changed in the GF mice compared to SPF mice (Fig. 2a, b). These data support the conclusion that the gut microbiota is dispensable for the development of natural IELs in the small intestine.

Since our data above showed that the innate sensory pathways specifically affected the natural IELs in the small intestine, we wondered whether food-derived triggers such as DNAs or RNAs contribute to the maintenance of the natural IELs. We first compared the development of natural IELs in the C57BL/6 mice fed a normal diet (ND) or a purified diet (PD, AIN-93G) devoid of nucleic acids (Supplementary Fig. 2a). C57BL/6 mice weaned on the purified diet were similar to standard chow diet mice in terms of weight gain, small intestine length, and serum nutritional biomarkers (Supplementary Fig. 2b–d). We discovered that the mice fed the purified diet had much lower levels of the natural IELs, although the number of the induced IELs was unaffected by the diet (Fig. 2c, d). We subsequently supplemented the purified diet with DNAs and RNAs (PD+NA) and found that this restored the natural IEL levels in their small intestine (Fig. 2e–g). The addition of nucleic acids did not affect the overall number of induced IELs ( $\text{TCR}\beta^+\text{CD8}\alpha\beta^+$ ), but the percentage of induced IELs rose due to a decrease in natural IELs (Fig. 2e–g). Given MAVS and STING's redundant roles in responding to dietary nucleic acids for natural IELs development, we found that adding DNAs or RNAs could sufficiently restore the number of natural IELs (Supplementary Fig. 2e). We further fed mice with another purified diet, AIN-93M, and obtained similar results as with AIN-93G (Supplementary Fig. 2f), suggesting that the observed phenotype is not related to probable differences in dietary components. Since dietary factors can activate the AhR signaling pathway to maintain natural IELs homeostasis<sup>23</sup>, we analyzed the AhR expression level in the whole tissue or in natural IELs, as well as its reaction in the small intestine. We found that both were not substantially different between the purified diet-fed mice and the normal diet-fed mice (Supplementary Fig. 2g, h), showing that the purified diet we utilized can normally activate the endogenous AhR pathway.

To evaluate whether food consumption in the small intestine is the primary contributor to nucleic acid levels, we examined nucleic

acid levels in the duodenal mucus of wild-type mice fed the normal diet or the purified diet, as well as mice fed the normal diet but fasting. We found that nucleic acid levels were much higher in mice fed the normal diet than in mice fed the purified diet (Supplementary Fig. 2i) or in the normal diet-fed mice under fasting (Supplementary Fig. 2j), demonstrating that the diet primarily regulates mucus nucleic acids. We then compared the topological distribution of dietary nucleic acids to commensal bacteria-derived nucleic acids in the small intestine *in situ*. We found that dietary nucleic acids were detectable in the mucus but not commensal bacteria-derived nucleic acids (Supplementary Fig. 2k, l). Although the microbiota communities of PD-fed mice and ND-fed mice differ in composition, the mice in the PD and PD+NA groups had a similar microbiota composition (Supplementary Fig. 2m), indicating that the nucleic acid supplementation does not markedly alter the microbiota and its effect on restoring the phenotype of natural IELs in the PD-fed mice may be microbiota independent. To further rule out the potential effect of microbiota-derived nucleic acids, we examined the natural IELs in GF mice fed a purified diet supplemented with or without nucleic acids. We observed similar results to the SPF condition (Supplementary Fig. 2n, o). Taken together, these data suggest that dietary nucleic acids, rather than microbiota, are critical for maintaining natural IELs.

Consistent with the microbiota-independent regulation of natural IELs, we discovered that the numbers of the natural IELs were similarly reduced in the MS DKO mice compared to wild-type control mice under both cohousing and separated housing conditions (Fig. 2h). As a recent study reported that commensal viruses affect the development of IELs<sup>24</sup>, we treated mice with the antiviral cocktail (AVC) employed in that study and found that the numbers of natural IELs were not changed while the numbers of induced IELs ( $\text{TCR}\alpha\beta^+\text{CD8}\alpha\beta^+$  IELs) was reduced after the cocktail treatment (Supplementary Fig. 2p), which is consistent with our results as well as the previous reports from GF mice studies<sup>16–18</sup>. To determine the effects of nucleic acid adaptors other than MAVS and STING on natural IELs, we fed MS DKO mice either the purified diet or the purified diet supplemented with nucleic acids. We found that the numbers of natural IELs were marginally lower in MS DKO mice given the purified diet compared to DKO mice fed the nucleic acid-supplemented diet (Fig. 2i), implying that other nucleic acid sensors are involved. Consistent with a previous report<sup>21</sup>, our study also demonstrated the role of MyD88 for natural IEL maintenance. Thus, we speculated that TLRs-MyD88 pathways may also be involved in the nucleic acid-mediated effects on natural IEL maintenance, which awaits further research. However, we found that the impacts of MAVS and STING-mediated pathways were greater than those of TLRs-MyD88 pathways. Collectively, our data suggest that food-derived DNAs and RNAs may trigger multiple innate sensing pathways to maintain natural IELs in the small intestine.

### Dietary nucleic acids promote the development of natural IELs through IL-15

To explore how the innate sensing pathways contribute to the natural IEL development, we first performed bone marrow (BM) transfer into  $\text{Rag1}^{-/-}$  mice and found that the loss of MAVS and STING in BM did not affect the percentages and numbers of the natural IELs (Supplementary Fig. 3a, b), indicating that the role of MAVS and STING in natural IEL development is IEL extrinsic. Furthermore, we conducted BM transfer experiments and found that the expression of STING and MAVS in non-hematopoietic cells were important for the percentages and numbers of the natural IELs (Fig. 3a). We then examined the early development of the natural IELs, and found that the percentages and numbers of the precursors (DN  $\text{TCR}\beta^+$ , representing  $\text{TCR}\alpha\beta^+\text{CD4}^+\text{CD8}\beta^-$ ) of the  $\text{TCR}\alpha\beta^+\text{CD8}\alpha\alpha^+$  IELs, were not changed in the thymus and small intestine of the MS DKO mice compared with wild-type control mice (Supplementary Fig. 3c, d), indicating that the innate sensing pathways did not affect the early development of

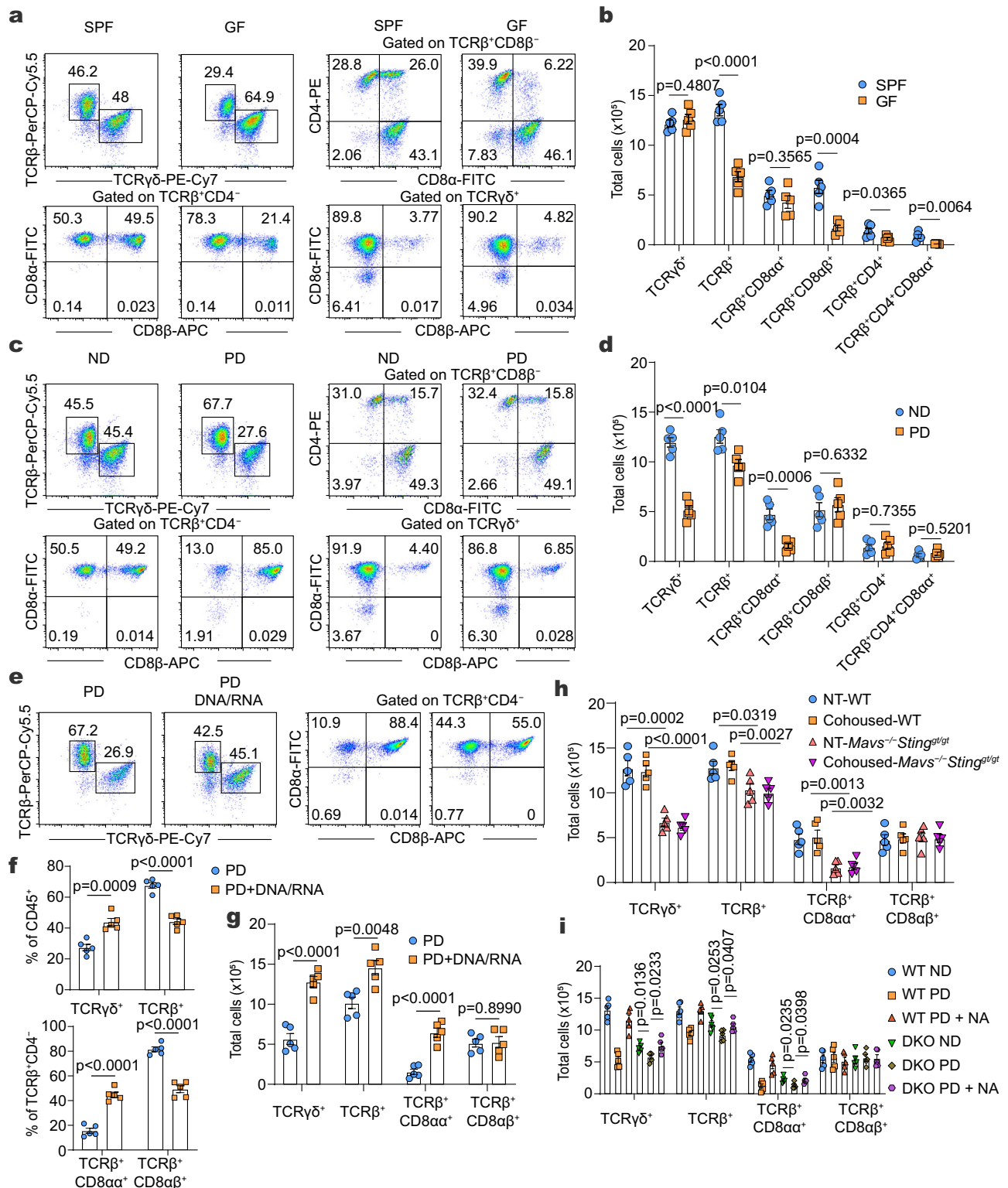


**Fig. 2 | Dietary nucleic acids promote the development of natural IELs in the small intestine.** **a, b** Representative flow plots (**a**) or cell numbers (**b**) of small intestinal IEL subsets from SPF or GF mice,  $n = 5$ . **c, d** Representative flow plots (**c**) or cell numbers (**d**) of small intestinal IELs from C57BL/6 mice fed normal diet (ND) or purified diet (PD) for 6 weeks after their weaning,  $n = 5$ . **e–g** Representative flow plots (**e**) or cell percentages (**f**) and cell numbers (**g**) of small intestinal IELs from C57BL/6 mice fed PD with or without supplement of 0.5% purified nucleic acids (0.25% purified salmon testes DNA and 0.25% purified yeast RNA, DNA/RNA) for 6 weeks after their weaning,  $n = 5$ . **h** The cell numbers of the indicated small

intestinal IEL subsets from wild type (WT) or *Mavs* $^{-/-}$ *Sting* $^{gt/gt}$  mice which were kept in separate cages (NT) or co-housed cages for 1 month,  $n = 5$ . **i** The absolute cell numbers of the indicated IEL subsets in the small intestine from WT mice or *Mavs* $^{-/-}$ *Sting* $^{gt/gt}$  mice fed ND or PD with or without a supplement of 0.5% purified nucleic acids for 6 weeks after their weaning,  $n = 5$ . Data are mean  $\pm$  s.e.m. and from one experiment representative of two (**a, b, h**, and **i**) or three independent experiments (**c–g**). Statistics: one-way ANOVA followed by the Bonferroni post hoc test (**h, i**) or two-tailed, Student's *t* tests (**b, d, f**, and **g**). Source data are provided as a Source Data file.



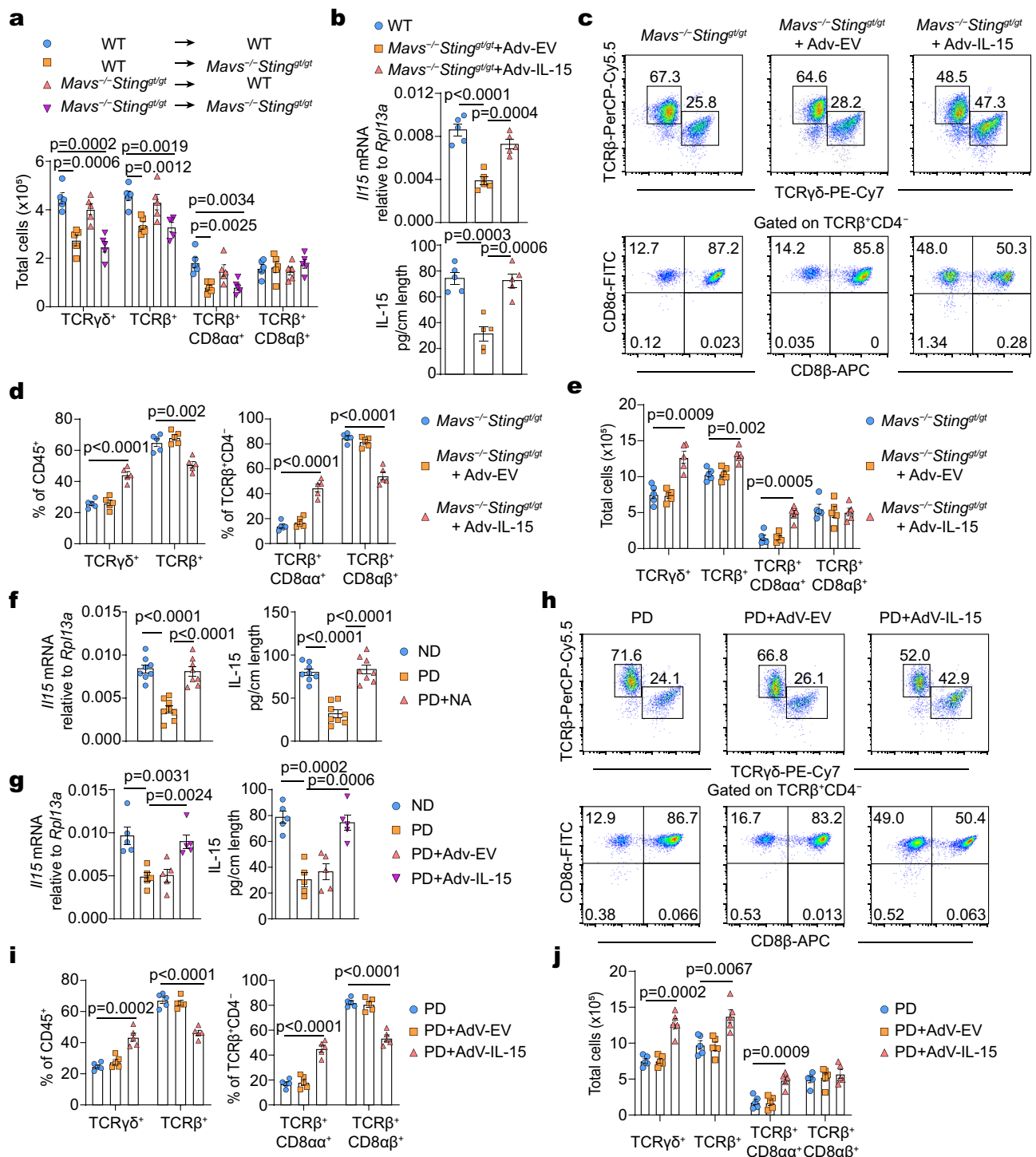


**Fig. 3 | Dietary nucleic acids maintain small intestine natural IELs via IL-15.**

**a** The absolute cell numbers of small intestinal IELs from the indicated BM chimeras of WT BM cells into irradiated WT or *Mavs*<sup>-/-</sup> *Sting*<sup>glt/glt</sup> mice, or of *Mavs*<sup>-/-</sup> *Sting*<sup>glt/glt</sup> BM cells into irradiated WT or *Mavs*<sup>-/-</sup> *Sting*<sup>glt/glt</sup> mice,  $n = 5$ . **b** Quantification of the expression of *Il15* at the mRNA level by qPCR or protein level by ELISA in the small intestine from WT or *Mavs*<sup>-/-</sup> *Sting*<sup>glt/glt</sup> mice intravenously injected with Adv-EV or Adv-IL-15 adenovirus,  $n = 5$ . **c–e** Representative flow plots (**c**) or cell percentages (**d**) and cell numbers (**e**) of small intestinal IELs from *Mavs*<sup>-/-</sup> *Sting*<sup>glt/glt</sup> mice treated with Adv-EV or Adv-IL-15 adenovirus,  $n = 5$ . **f** Quantification of the expression of *Il15* at the mRNA level by qPCR or protein level by ELISA in the small intestine from C57BL/

6 mice fed ND or PD with or without supplement of 0.5% purified nucleic acids,  $n = 8$ . **g** Quantification of the expression of *Il15* at the mRNA level by qPCR or protein level by ELISA in the small intestine from C57BL/6 mice that were pre-fed ND or PD, and then intravenously injected with or without Adv-EV or Adv-IL-15 adenovirus,  $n = 5$ . **h–j** Representative flow plots (**h**) or cell percentages (**i**) and cell numbers (**j**) of small intestinal IELs from C57BL/6 mice that were fed PD and treated with Adv-EV or Adv-IL-15 adenovirus,  $n = 5$ . Data are mean  $\pm$  s.e.m. and from one experiment representative of two (**a**, **b**, **f**, **g**) or three independent experiments (**c–e**, **h–j**). Statistics: one-way ANOVA followed by the Bonferroni post hoc test (**a**, **b**, **d**, **g**, **i**, **j**). Source data are provided as a Source Data file.

natural IELs or their recruitment to the small intestine. We further observed that MAVS and STING deficiency reduced natural IEL proliferation while increasing natural IEL death (Supplementary Fig. 3e). These results suggest that innate sensing in the small intestine may promote natural IEL accumulation by inducing proliferation or survival factors.

IL-15, TGF- $\beta$ 1, and IL-7 are the key microenvironment cytokines for IEL proliferation and survival<sup>14</sup>. We found that IL-15 mRNA and protein levels were significantly decreased in the small intestine of the MS DKO mice (Supplementary Fig. 3f), while the mRNA levels of TGF- $\beta$ 1 and IL-7 remained unchanged (Supplementary Fig. 3g), suggesting that IL-15 production via MAVS and STING pathways is involved in IEL development. We subsequently tested whether IL-15 produced from hematopoietic cells or non-hematopoietic cells contributes to natural IEL proliferation by performing bidirectional BM transfer experiments with *IL15*-deficient mice. We discovered that hematopoietic cell-derived IL-15 was not essential for the maintenance of natural IELs (Supplementary Fig. 3h, i), which is consistent with previous reports<sup>25,26</sup>. Meanwhile, we observed that IL-15 production is reduced in epithelial cells from MS DKO mice compared to WT mice (Supplementary Fig. 3j).

To determine whether the observed partial reduction (about half the amount) of IL-15 could contribute to the IEL phenotype in MS DKO mice, we generated *IL15*<sup>-/-</sup> mice, and found that the small intestinal IL-15 protein level was partially reduced while the frequency and number of natural IELs were also greatly reduced in these mice compared with wild-type control mice (Supplementary Fig. 3k–m), indicating that the development of natural IELs may be highly dependent on IL-15 levels. In addition, we compared the roles of MyD88 versus MAVS and STING-mediated signaling in IL-15 production and found that the decrease of IL-15 levels in MyD88 KO mice is less than that in MS DKO mice (Supplementary Fig. 3n), which is consistent with the differentially reduced levels of natural IELs in these mice as described above. Furthermore, we found that dietary nucleic acids might modulate IL-15 production in GF mice fed the purified diet supplemented with or without nucleic acids (Supplementary Fig. 3o).

To further demonstrate whether the reduced IL-15 level leads to a reduction in the number of the natural IELs, we established the adenoviral expression system to exogenously express IL-15 in mice in vivo and found that the system could successfully restore the reduced IL-15 level in MS DKO mice (Fig. 3b). Indeed, increasing IL-15 expression level in these mice to that of wild-type mice restored the reduced percentage and number of the natural IELs (Fig. 3c–e), supporting the conclusion that MAVS and STING-mediated IL-15 expression is critical for the development of natural IELs in the small intestine.

Consistently, we found that IL-15 mRNA and protein levels were significantly reduced in the small intestine of the purified diet-fed mice than in normal diet-fed mice, while adding DNAs and RNAs into the purified diet restored IL-15 levels (Fig. 3f). We then utilized the adenoviral expression system to express IL-15 in the purified diet-fed mice (Fig. 3g), and found that the restoration of IL-15 levels in these mice rescued the reduced percentages and numbers of the natural IELs (Fig. 3h–j). The IL-15 levels had no effect on the numbers of the induced IELs (Fig. 3j), whereas the reduced percentages of induced IELs caused by the IL-15 rise were attributed to the increased percentages of the natural IELs (Fig. 3i). These data suggest that food-derived nucleic acids, which activate MAVS and STING pathways, induce IL-15 expression to maintain natural IELs.

Since TBK1 is a key downstream kinase for MAVS and STING signaling, we investigated whether it is required for the reduced natural IEL phenotype. To explore the in vivo function of TBK1, we generated *Tnfr $\alpha$* <sup>-/-</sup>*Tbk1*<sup>-/-</sup> mice as *Tbk1*<sup>-/-</sup> mice are embryonic lethal<sup>27</sup>. Consistent with the data observed in MS DKO mice, the *Tnfr $\alpha$* <sup>-/-</sup>*Tbk1*<sup>-/-</sup> mice had reduced IL-15 mRNA and protein production in the small intestine compared to that in the *Tnfr $\alpha$* <sup>-/-</sup> mice (Fig. 4a, b). TBK1 deficiency also

resulted in a reduction in the percentage and number of the natural IELs (Fig. 4c–e). Given the MAVS and STING-mediated innate sensing pathways can induce type I interferons that promote IL-15 expression<sup>28</sup>, we next determined whether TBK1 signaling controls IL-15 production and natural IEL development in mice via type I interferons. However, we found that loss of *Irfnb1* or *Irfnar1* (a shared receptor for both interferon- $\beta$  and all interferon- $\alpha$ s) did not influence the levels of IL-15 mRNA and protein in the small intestine at steady state (Fig. 4f, g), similar with a recent report<sup>24</sup>. The percentages and numbers of the natural IELs were also unchanged in the *Irfnb1*- or *Irfnar1*-deficient mice (Fig. 4h–j). We further found that *Irfnar1*-deficient mice fed the purified diet had lower IL-15 protein levels than mice fed the normal diet, while the addition of DNAs and RNAs to the purified diet restored the reduced IL-15 production (Fig. 4k). Taken together, our results show that dietary nucleic acids activate MAVS and STING signaling pathways to maintain natural IELs in a TBK1-dependent but IFNs-independent manner.

### Dietary nucleic acids promote protein antigen-induced oral tolerance

Pretreatment with protein antigen is well recognized to induce oral tolerance to subsequent protein antigen stimulation<sup>5</sup>. It is also known that nucleic acids, such as those found in adjuvants, can promote protein antigen-induced immune responses<sup>29,30</sup>. We studied whether dietary nucleic acids could promote oral tolerance. To test this, we examined low-dose OVA (protein antigen)-induced oral tolerance in C57BL/6 mice fed the normal diet or the purified diet lacking nucleic acids. We found that in the normal diet-fed mice, oral OVA pretreatment strongly induced tolerance to OVA, as evidenced by the suppression of the footpad delayed-type hypersensitivity (DTH) response (Fig. 5a and Supplementary Fig. 4a), decreased production of IFN- $\gamma$  and IL-2 in splenocytes when restimulated with OVA in vitro (Fig. 5b), and reduced levels of OVA-specific IgE, IgG1, and IgG2a antibodies in serum after OVA sensitization (Fig. 5c). However, OVA-induced oral tolerance was impaired in mice fed the purified diet (Fig. 5a–c).

To determine whether the impaired oral tolerance is caused by a lack of food-derived nucleic acids, we then compared the OVA-induced tolerance in C57BL/6 mice pre-fed the purified diet or the purified diet supplemented with nucleic acids (DNAs and RNAs). We observed that nucleic acid supplementation restored the impaired OVA-induced oral tolerance (Fig. 5a–c), implying that dietary nucleic acids promote protein antigen-induced oral tolerance. Since there are numerous oral tolerance induction protocols<sup>31</sup>, we investigated whether oral tolerance is impaired in PD-fed mice with high-dose ingested antigens. However, we found that oral tolerance could still be established in PD-fed mice with a single high-dose gavage of 25 mg OVA (Supplementary Fig. 4b–d). Multiple mechanisms may be involved in the induction of tolerance by different protocols, for example, low doses of antigen favor active suppression by inducing antigen-specific Tregs whereas higher doses of antigen favor clonal anergy or deletion<sup>6</sup>. Thus, natural IELs regulate the induction of low-dose antigen-induced oral tolerance but are not essential participants in the induction of systemic unresponsiveness to high doses of orally ingested antigen. Consistent with this, we obtained similar results in another low-dose OVA-induced OVA/cholera toxin allergy model (Supplementary Fig. 4e–g). At the same time, we found that in another study based on the AIN-93G diet but with changes in fiber content, the purified diet had minimal effect on the peanut extract-induced food allergy<sup>32</sup>, indicating that the nucleic acid-dependent establishment of oral tolerance is likely context-dependent. As microbiota has been reported to play a role in the induction of oral tolerance<sup>33</sup>, we performed fecal transplantation experiments and found that the effects of dietary nucleic acids on the OVA-induced oral tolerance were not related to potential changes in microbiota (Supplementary Fig. 4h–k).

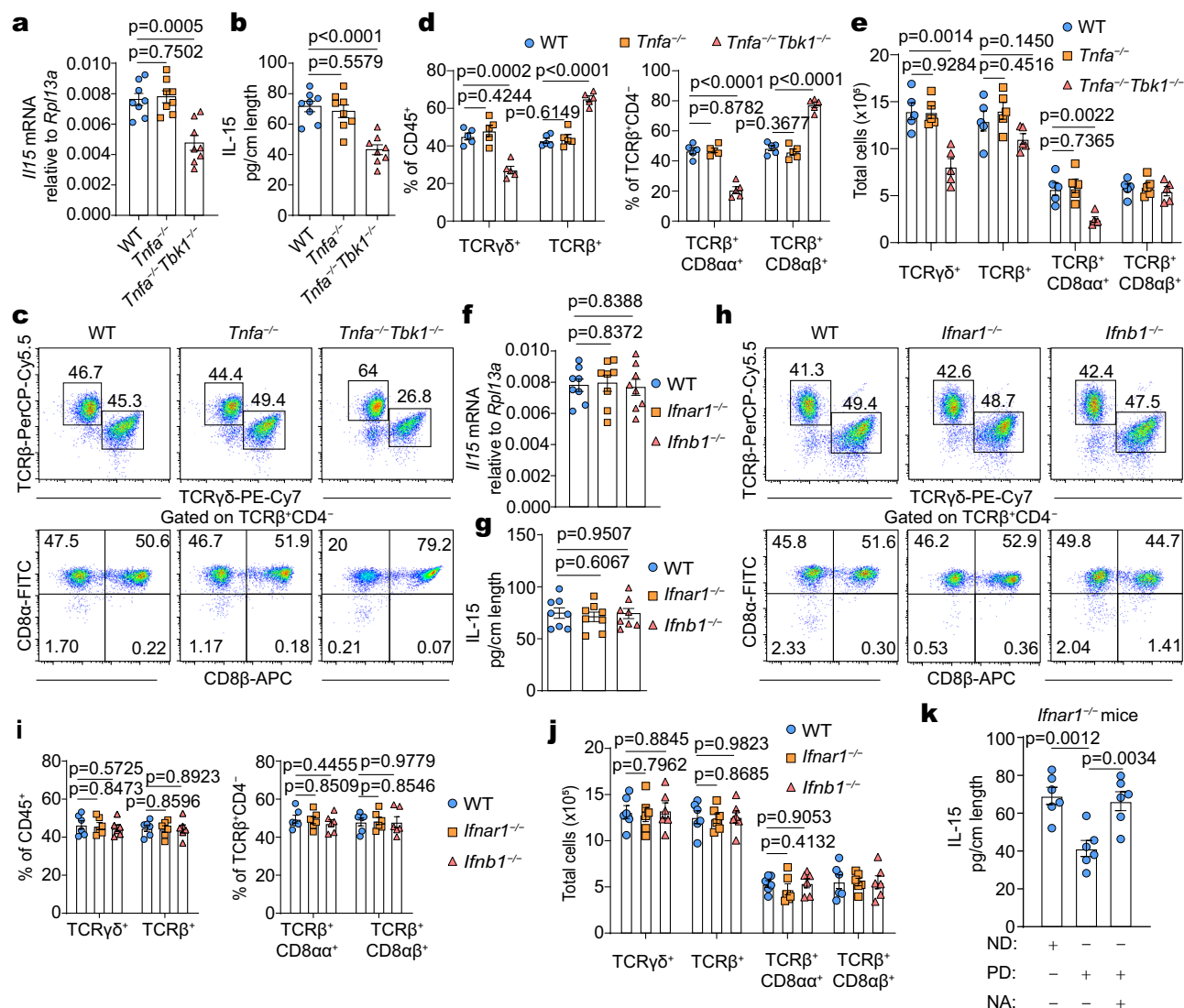


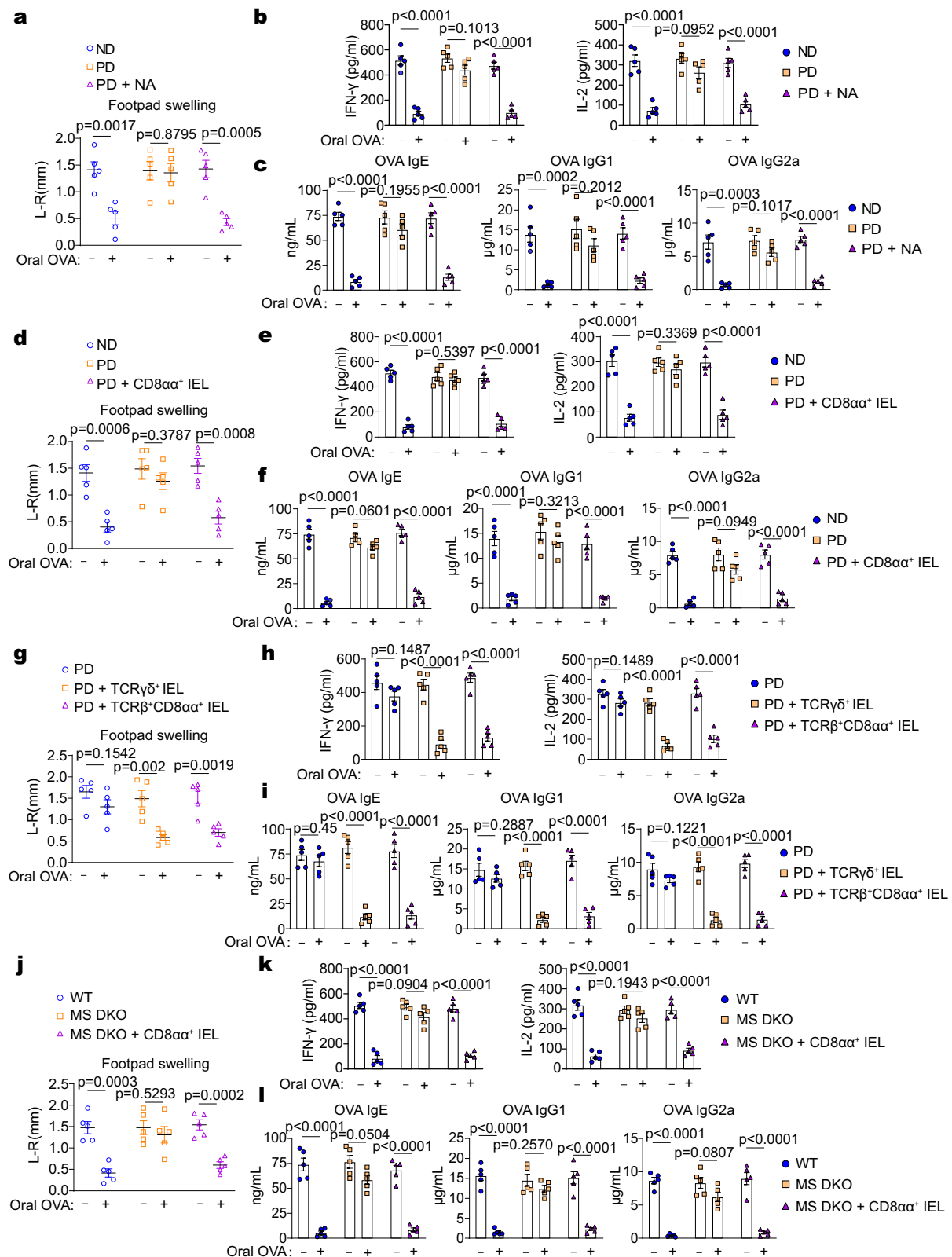
**Fig. 4 | MAVS and STING signaling pathways maintain natural IELs in a TBK1-dependent but IFN-I-independent manner. a, b** Quantification of the expression of *Il15* at the mRNA level by qPCR (a) or protein level by ELISA (b) in the small intestine from WT, *Tnfa*<sup>-/-</sup>, or *Tnfa*<sup>-/-</sup>*Tbk1*<sup>-/-</sup> mice,  $n=8$ . **c–e** Representative flow plots (c), cell percentages (d) and cell numbers (e) of small intestinal IELs from WT, *Tnfa*<sup>-/-</sup>, or *Tnfa*<sup>-/-</sup>*Tbk1*<sup>-/-</sup> mice,  $n=5$ . **f, g** Quantification of the expression of *Il15* at the mRNA level by qPCR (f) or protein level by ELISA (g) in the small intestine from WT, *Ifnar1*<sup>-/-</sup> or *Ifnb1*<sup>-/-</sup> mice,  $n=8$ . **h–j** Representative flow plots (h), cell percentages (i)

and cell numbers (j) of small intestinal IELs from WT, *Ifnar1*<sup>-/-</sup> or *Ifnb1*<sup>-/-</sup> mice,  $n=6$ . **k** Quantification of the expression of IL-15 by ELISA in the small intestine from *Ifnar1*<sup>-/-</sup> mice fed ND or PD with or without supplement of 0.5% purified nucleic acids (NA),  $n=6$ . Data are shown as mean  $\pm$  s.e.m. and from one experiment representative of two (a, b, f, g, k) or three independent experiments (c–e, h–j). The  $P$  values were determined using one-way ANOVA followed by the Bonferroni post hoc test (a, b, d–g, i–k). Source data are provided as a Source Data file.

The TCR $\gamma\delta^+$  natural IELs have been shown to promote oral tolerance<sup>34–37</sup>. To determine whether the dietary nucleic acid-maintained natural IELs contribute to protein antigen-induced oral tolerance, C57BL/6 mice were first fed the purified diet and then adoptively transferred with the natural IELs (TCR $\alpha\beta^+$ CD8 $\alpha\alpha^+$  and TCR $\gamma\delta^+$ ). We discovered that transferring natural IELs restored the impaired OVA-induced oral tolerance in the purified diet-fed mice (Fig. 5d–f and Supplementary Fig. 4l–n). To determine whether these transplanted natural IELs could return to the intestine to function, we transferred the mice with  $\beta 7$ -deficient natural IELs, which lack the expression of  $\alpha_E\beta 7$  integrin for their intestinal homing and retention<sup>38</sup>. We found that  $\beta 7$ -deficient natural IELs failed to rescue the impaired OVA-induced oral tolerance in the purified diet-fed mice (Supplementary Fig. 4o–q). This suggests that natural IELs' intestinal homing capabilities are essential for oral tolerance. To further clarify which subset of natural IELs is essential for the establishment of oral

tolerance, we individually sorted TCR $\gamma\delta^+$  IELs or TCR $\alpha\beta^+$  IELs and then transferred them into the PD-fed mice, followed by oral tolerance induction. We found that these two types of natural IELs have similar rescue effects on the phenotype (Fig. 5g–i). In fact, both previous microarray assays and recent single-cell sequencing data have indicated that these two kinds of cell populations have high similarities in gene expression features<sup>37,39</sup>.

To further test the hypothesis that dietary nucleic acids promote protein antigen-induced oral tolerance through innate sensing pathways, we studied MS DKO mice in OVA-induced oral tolerance and discovered it was impaired in the DKO mice compared to the co-housed WT mice (Fig. 5j–l). We also conducted fecal transplantation experiments to exclude the potential effects of microbiota on oral tolerance given the deficiency of both genes (Supplementary Fig. 5a–c). Consistent with the effects of natural IELs in the dietary nucleic acid-promoted oral tolerance, we found



that adoptive transfer of WT but not the  $\beta 7$ -deficient natural IELs restored defective OVA-induced oral tolerance in the double-deficient mice (Fig. 5j–l and Supplementary Fig. 5d–g). Given *Il15*<sup>+/-</sup> mice have a similar phenotype of reduced natural IELs to MS DKO mice or PD-fed mice, we examined the oral tolerance model in *Il15*<sup>+/-</sup> mice and found that oral tolerance is also compromised (Supplementary Fig. 5h–j). Taken together, our findings suggest that dietary

nucleic acids activate innate sensing pathways to maintain natural IELs for oral tolerance.

### Natural IELs-derived TGF- $\beta 1$ promote OVA-induced oral tolerance

It is unclear how natural IELs function in oral tolerance, although they have been reported to have an immunoregulatory gene profile that



**Fig. 5 | Dietary nucleic acids promote protein antigen (OVA)-induced oral tolerance through natural IELs.** **a–c** C57BL/6 mice pre-fed ND or PD without or with NA (0.5% purified nucleic acids) for 6 weeks after their weaning followed by induction of OVA-mediated oral tolerance, then DTH responses were measured (**a**), the effector cytokines of total spleen cells (**b**) or serum OVA-specific antibody levels (**c**) were analyzed by ELISA,  $n = 5$ . **d–f** C57BL/6 mice pre-fed ND or PD for 6 weeks after their weaning, transferred with or without natural CD8 $\alpha\alpha^+$  IELs in the last 2 weeks, and then followed by induction of OVA-mediated oral tolerance ( $n = 5$ ), then DTH responses were measured (**d**), the effector cytokines of total spleen cells (**e**) or serum OVA-specific antibody levels (**f**) were analyzed,  $n = 5$ . **g–i** PD-fed mice

transferred with TCR $\gamma\delta^+$  IELs or TCR $\beta^+$ CD8 $\alpha\alpha^+$  IELs followed by OVA-mediated oral tolerance, then DTH responses were measured (**g**), the effector cytokines of total spleen cells (**h**) or serum OVA-specific antibody levels (**i**) were analyzed,  $n = 5$ . **j–l** WT or MS DKO mice transferred with or without natural CD8 $\alpha\alpha^+$  IELs followed by OVA-mediated oral tolerance, then DTH responses were measured (**j**), the effector cytokines of total spleen cells (**k**) or serum OVA-specific antibody levels (**l**) were analyzed,  $n = 5$ . Data are mean  $\pm$  s.e.m. and from one experiment representative of two independent experiments (**a–l**). Statistics: two-tailed Student's  $t$  test. Source data are provided as a Source Data file.

includes TGF- $\beta$  family genes<sup>8,40</sup>. To determine the potential roles of natural IELs-derived TGF- $\beta$ s, we first sorted out natural IELs, induced IELs, and IECs to compare their expression levels of TGF- $\beta$  family members, and found that natural IELs had high expression of TGF- $\beta$ 1 and TGF- $\beta$ 3 (Supplementary Fig. 6a), which could be further up-regulated after the OVA antigen feeding (Supplementary Fig. 6b, c). We then examined the MS DKO mice or the purified diet-fed mice, and found that small intestinal *Tgfb1* and *Tgfb3* were not up-regulated in these mice compared to respective control mice in early time points after OVA feeding, but their upregulation could be fully restored with the transfer of natural IELs (Supplementary Fig. 6d, e). These data suggest that natural IELs are critical for TGF- $\beta$ 1 and TGF- $\beta$ 3 induction at the early phase of oral tolerance.

Considering that the natural IELs were not totally lost in the MS DKO or PD mice at steady state while the induction of TGF- $\beta$ s was almost completely blocked in these mice in the OVA tolerance model, we determined whether the remaining IELs have reduced expression of TGF- $\beta$ s. However, we found that there was no difference in the expression of *Tgfb1* and *Tgfb3* of the natural IELs from WT, MS DKO, or PD-fed mice at steady state (Supplementary Fig. 6f), suggesting that the reduced expression of the initial TGF- $\beta$ s due to the reduced number of natural IELs may have an amplifying effect on their own induction later in the tolerance model. It's known that TGF- $\beta$  can upregulate TGF- $\beta$ -activating integrins (*Itgav*, *Itgb6*, *Itgb8*) which mediate the release of TGF- $\beta$  to produce bioactive TGF- $\beta$ <sup>41–43</sup>. Then, we sorted natural IELs from WT mice and treated them with TGF- $\beta$ 1 or TGF- $\beta$ 3 to test their ability to give favorably feedback on themselves in the initial niche environment. The treatments led to enhanced expression of TGF- $\beta$ -activating integrins (Supplementary Fig. 6g). Consistently, the expression of the TGF- $\beta$ -activating integrins and the secreted TGF- $\beta$ s were lower in the natural IELs from MS DKO or the PD mice (Supplementary Fig. 6h, i). Additionally, when these natural IELs isolated from the MS DKO mice were stimulated by TGF- $\beta$  in vitro, they could similarly upregulate the expression of the TGF- $\beta$ -activating integrins (Supplementary Fig. 6j). Taken together, these results indicate that the initial natural IEL-derived TGF- $\beta$ s can positively amplify their production in the local niche microenvironment. We then wondered whether natural IELs-derived TGF- $\beta$ s might play a role in OVA-induced oral tolerance. To elucidate which TGF- $\beta$  is engaged in the oral tolerance, we used ex vivo CRISPR-Cas9 gene targeting method to individually knockout the TGF- $\beta$ 1 or TGF- $\beta$ 3 in natural IELs (Fig. 6a, b). We found the transfer of wild-type or TGF- $\beta$ 3-deficient natural IELs but not the TGF- $\beta$ 1-deficient natural IELs could restore defective oral tolerance phenotype in the MS DKO mice (Fig. 6c–e) or the purified diet-fed mice (Fig. 6f–h). Taken together, our results suggest that natural IELs-derived TGF- $\beta$ 1 promotes OVA-induced oral tolerance.

### Natural IELs promote the development of antigen-specific Treg cells for OVA-induced oral tolerance

It remains unclear how natural IELs-derived TGF- $\beta$ 1 supports the induction of oral tolerance. Treg cells play a significant function in oral tolerance<sup>7,44</sup>. Tolerogenic dendritic cells (DC), particularly CD103 $^+$  DC, can capture exogenous antigens in the gut and then drain to the

mesenteric lymph node to promote the development of antigen-specific Treg cells<sup>45–47</sup>. Therefore, we determined whether natural IELs-derived TGF- $\beta$ 1 affects the development or function of the migratory CD103 $^+$  DCs. We found that the number and frequency of the migratory CD103 $^+$  DCs were not changed in the small intestine LP and MLN in the MS DKO mice or the purified diet-fed mice compared to their respective control mice during OVA-induced oral tolerance (Supplementary Fig. 7a–d). To gain insight into the impact of the decreased natural IELs on small intestinal CD103 $^+$  DCs during oral tolerance, we performed transcriptomic analysis of LP CD103 $^+$  DCs enriched from the entire small intestine (including the duodenum, jejunum, and ileum) of WT mice before or during oral tolerance induction. In vivo, OVA treatment dramatically increased the expression of over 300 genes in CD103 $^+$  DCs. Notably, the TGF- $\beta$ -activating integrin *Itgb8* was dramatically upregulated (Fig. 7a). Integrin  $\beta$ 8 has been reported to be vital for the CD103 $^+$  DCs to produce bioactive TGF- $\beta$  to promote the induction of antigen-specific Tregs<sup>48–50</sup>, and its expression is acquired in the small intestine by local signals, particularly TGF- $\beta$ 1<sup>42</sup>. We found that integrin  $\beta$ 8 was up-regulated in the CD103 $^+$  DCs after OVA oral gavage, which was inhibited in MS DKO mice or purified diet-fed mice (Fig. 7b, c). We further found that the transfer of wild-type natural IELs but not the TGF- $\beta$ 1-deficient natural IELs restored defective upregulation of integrin  $\beta$ 8 (Fig. 7b, c), suggesting that TGF- $\beta$ 1 derived from natural IELs promote the function of the migratory CD103 $^+$  DCs. The migratory intestinal CD103 $^+$  DCs are critical for the development of the induced Tregs in the oral tolerance model<sup>46</sup>. Next, we investigated whether natural IELs could promote the development of antigen-specific Treg cells for OVA-induced oral tolerance. To do this, we adoptively transplanted naïve CD45.1 $^+$  OT-II cells into CD45.2 $^+$  wild-type (WT) or MS DKO recipient mice, then treated them with oral OVA for one week. We then assessed the antigen-specific Treg cells at both systemic and mucosal sites. We found that the cell frequencies of both systemic and mucosal antigen-specific Treg cells were significantly increased in WT recipient mice, whereas they were blocked in the MS DKO recipient mice (Fig. 7d, e and Supplementary Fig. 7e). Similarly, purified diet-fed recipient mice showed lower upregulation of antigen-specific Treg cell frequencies than normal diet-fed recipient mice (Fig. 7f, g). Next, we determined whether the adoptive transfer of WT natural IELs back into the aforementioned recipient mice could rescue the impaired development of oral OVA-induced Treg cells. Indeed, we found that the transfer of WT but not TGF- $\beta$ 1-deficient natural IELs restored the impaired frequencies of systemic and mucosal antigen-specific Treg cells in the MS DKO recipient mice (Fig. 7h, i) or the purified diet-fed recipient mice (Fig. 7j, k). These results indicate that TGF- $\beta$ 1 derived from small intestinal natural IELs activates tolerogenic CD103 $^+$  DCs in the MLN, leading to the development of antigen-specific Treg cells and modulating OVA-induced oral tolerance. In addition, to directly examine the interaction of CD103 $^+$  DCs with antigen-specific Treg cells, we sorted LP CD103 $^+$  DCs from DKO mice or PD-fed mice transferred with WT and *Tgfb1*-deficient natural IELs during oral tolerance induction and added them in co-culture with naïve OT-II cells. We observed that the DCs from DKO mice or PD-fed mice transferred with WT but not *Tgfb1*-deficient IELs could promote OT-II Treg differentiation in vitro (Supplementary Fig. 7f, g). As different cell types in

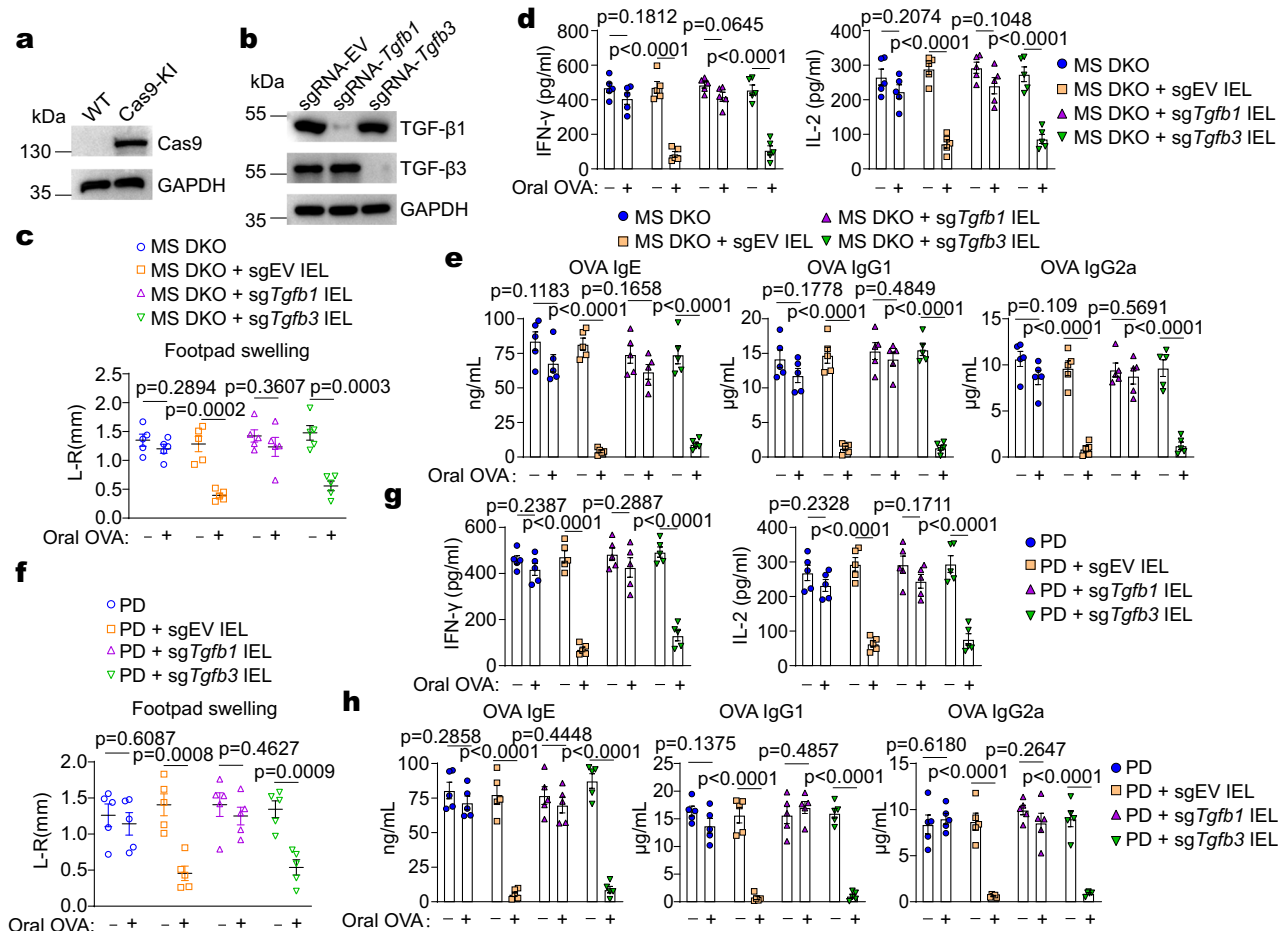


**Fig. 6 | Natural IELs-derived TGF- $\beta$ 1 promote OVA-induced oral tolerance.**

**a** Immunoblot analysis of the expression of transgenic CRISPR-Cas9 in natural CD8 $\alpha^+$  IELs. **b** Immunoblot analysis of the expression of TGF- $\beta$ 1 and TGF- $\beta$ 3 in natural CD8 $\alpha^+$  IELs by sgRNA-targeted knock-down. **c–e** MS DKO mice were first transferred without or with sgEV, sgTgfb1, or sgTgfb3 natural CD8 $\alpha^+$  IELs followed by induction of OVA-mediated oral tolerance ( $n = 5$ ), then DTH responses were measured (**c**), the effector cytokines of total spleen cells (**d**) or serum OVA-specific antibody levels (**e**) were analyzed. **f–h** C57BL/6 mice that were pre-fed PD for

6 weeks after their weaning, then transferred without or with sgEV, sgTgfb1, or sgTgfb3 natural CD8 $\alpha^+$  IELs in the last 2 weeks, and followed by induction of OVA-mediated oral tolerance ( $n = 5$ ), then DTH responses were measured (**f**), the effector cytokines of total spleen cells (**g**) or serum OVA-specific antibody levels (**h**) were analyzed. Data are mean  $\pm$  s.e.m. and from one experiment representative of two (**a**, **b**) or three (**c–h**) independent experiments. Statistics: two-tailed Student's  $t$  test. Source data are provided as a Source Data file.

the gut can produce and respond to TGF- $\beta$  to fulfill their own function<sup>51</sup>, our data suggest that natural IELs-derived TGF- $\beta$ 1 likely plays a niche-dependent role at the early phase of oral tolerance.

## Discussion

Oral tolerance to dietary antigens is critical to maintaining intestinal homeostasis. Previous studies have demonstrated that food-derived protein antigens play an essential role in oral tolerance<sup>6,7</sup>. We wondered whether other food-derived immune activators, such as nucleic acids, are involved in the establishment and maintenance of oral tolerance. We found that dietary nucleic acids, including RNAs and DNAs, activate innate sensing pathways to maintain natural IELs and consequently promote protein antigen-driven oral tolerance. Our study demonstrates the key role of dietary nucleic acids in the establishment and maintenance of oral tolerance and gut homeostasis.

While microbiota is essential for the development and maintenance of the induced IELs, including TCR $\alpha\beta^+$ CD4 $^+$  and TCR $\alpha\beta^+$ CD8 $\alpha\beta^+$  T cells<sup>18</sup>, it is dispensable for the development and maintenance of the natural IELs consisting of TCR $\alpha\beta^+$ CD8 $\alpha\alpha^+$  and TCR $\gamma\delta^+$ CD8 $\alpha\alpha^+$  T cells<sup>16–18</sup>. Nevertheless, an early report made the controversial claim that microbiota contributes to natural IEL accumulation<sup>22</sup>. This early report used crude cell gating strategies to

analyze different subsets of TCR $\beta^+$  IELs. At that time, it was not recognized that TCR $\beta^+$ CD4 $^+$ CD8 $\alpha\alpha^+$  IELs were induced IELs rather than natural IELs. Considering that TCR $\beta^+$ CD4 $^+$ CD8 $\alpha\alpha^+$  IELs are microbiota-dependent and that this report did not use CD4 $^+$  staining to exclude TCR $\beta^+$ CD4 $^+$ CD8 $\alpha\alpha^+$  IELs from the TCR $\beta^+$ CD8 $\alpha\alpha^+$  IELs, the observed reduction of TCR $\beta^+$ CD8 $\alpha\alpha^+$  IELs in GF mice could be due to the contribution of reduced TCR $\beta^+$ CD4 $^+$ CD8 $\alpha\alpha^+$  IELs. Furthermore, this study did not evaluate TCR $\gamma\delta^+$ CD8 $\alpha\alpha^+$  IELs, the major natural IEL population. We included the gating of CD4 $^+$  IELs in our GF mouse study and showed that the development and maintenance of the natural IELs are independent of the gut microbiota. Consistently, the natural IELs are mainly located in the small intestine with a low microbial load<sup>19</sup>, implying that local factors in the small intestine contribute to their development and maintenance. We employed a purified diet to demonstrate that food-derived nucleic acids promote the development and maintenance of the natural IELs, specifically in the small intestine but not in the colon. The specific effect of food-derived factors in the small intestine has also been documented in the modulation of regulatory T cells (Treg) by dietary antigens<sup>52</sup>, suggesting that dietary immune activators may function primarily in the small intestine, where nutrients are actively absorbed. Similarly, an earlier study showed that supplementation of nucleotides in the purified diet could

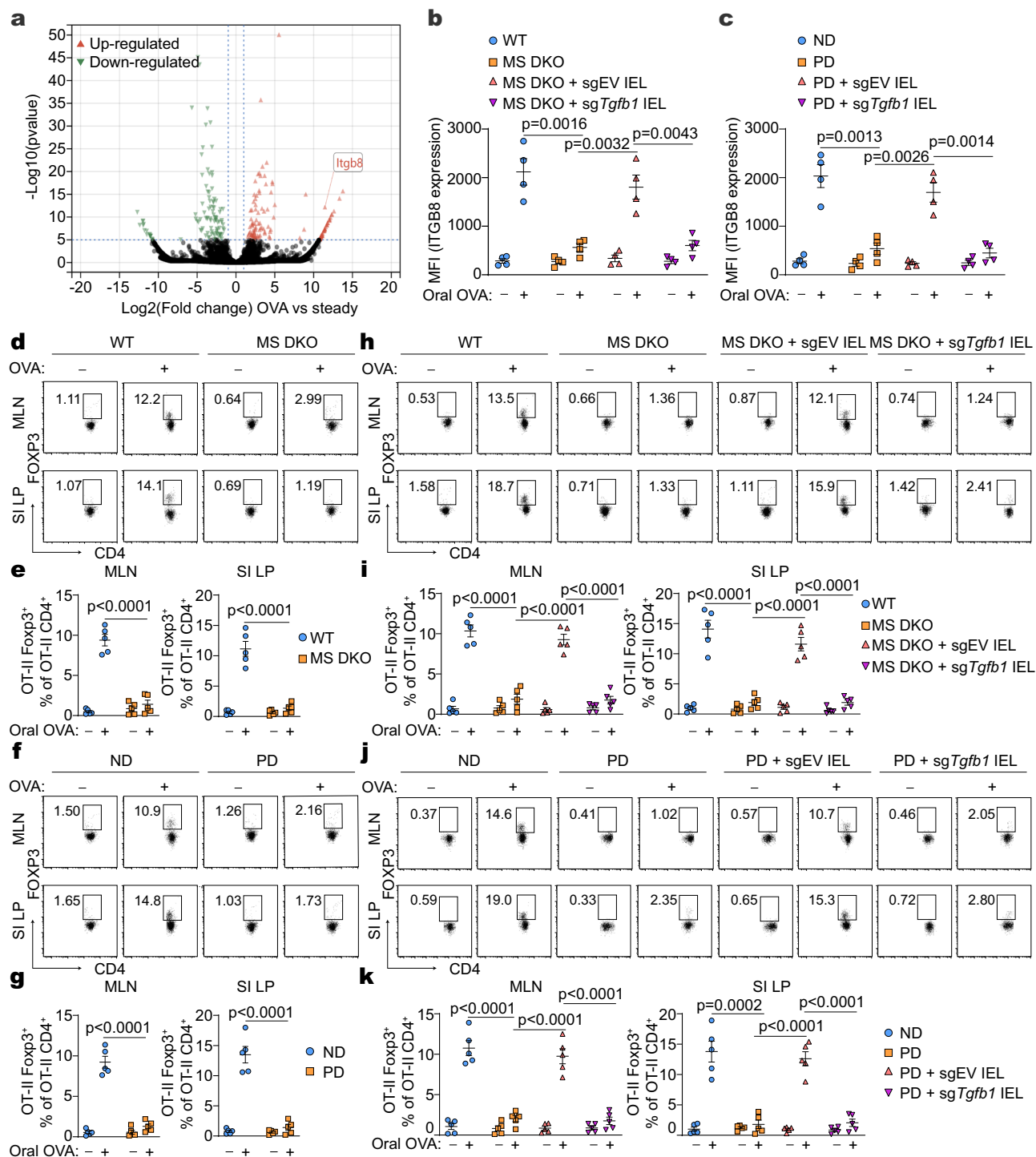


**Fig. 7 | Natural IELs promote the development of antigen-specific Tregs for OVA-induced oral tolerance through CD103<sup>+</sup> DCs.** **a** Volcano map of differentially expressed genes (*p* value < 0.01 and Log<sub>2</sub> fold change > 1) in small intestine lamina propria CD103<sup>+</sup> DCs sorted from WT mice at steady conditions or after OVA gavage for 3 days. **b, c** Flow cytometry analysis of  $\beta$ 8 expression in sorted small intestinal CD103<sup>+</sup>CD11b<sup>+</sup> DCs from below mice (*n* = 4) treated with or without OVA for three days. WT mice and MS DKO mice that were first transferred without or with sgEV or *sgTgfb1* natural CD8 $\alpha\alpha$ <sup>+</sup> IELs (**b**); ND or PD pre-fed C57BL/6 mice that were first transferred without or with sgEV or *sgTgfb1* natural CD8 $\alpha\alpha$ <sup>+</sup> IELs (**c**). **d–k** Flow analysis of percentages of OVA-specific Tregs in the mesenteric lymph node (MLN)

or small intestine lamina propria (SI LP) from below mice transferred with CD45.1<sup>+</sup> OT-II cells, followed by orally treated with OVA or PBS for one week (*n* = 5). Representative flow plots and cell percentages were shown. WT and MS DKO mice (**d, e**); ND or PD pre-fed C57BL/6 mice (**f, g**); WT mice and MS DKO mice that were first transferred without or with sgEV or *sgTgfb1* natural CD8 $\alpha\alpha$ <sup>+</sup> IELs (**h, i**); ND or PD pre-fed C57BL/6 mice that were first transferred without or with sgEV or *sgTgfb1* natural CD8 $\alpha\alpha$ <sup>+</sup> IELs (**j, k**). Data are mean  $\pm$  s.e.m. and from one experiment representative of two independent experiments. Statistics: two-tailed Student's *t* test (**b, c, e, j, i, k**). Source data are provided as a Source Data file.

promote the development of TCR $\gamma\delta^+$  IELs by boosting IL-7 production in intestine epithelial cells<sup>53</sup>. Given the differences in mouse strains and nucleic acids formula between their experimental system and ours, we hypothesize that there would be some variations between these two strains in how they respond to dietary nucleic acids or nucleotides for the maintenance and development of natural IELs.

Since exogenous nucleic acids can activate many RNA and DNA sensors<sup>54</sup>, we took advantage of the genetic deficiency of their downstream key adaptors (MyD88, TRIF, MAVS, and STING) to determine the downstream events mediated by dietary nucleic acids. We found that MAVS and STING redundantly maintain the development of the natural IELs, specifically in the small intestine but not in the colon. Although a recent study showed that *Mavs*-deficient mice had reduced numbers of both induced IELs and natural IELs<sup>24</sup>, we did not observe any changes in both IELs in *Mavs*-deficient mice housed in our facility. We further demonstrated that both DNAs and RNAs activated the MAVS/STING-TBK1 axis to induce IL-15 expression independently of the MAVS/STING type I interferon axis. IL-15 has been shown to play a critical role in the development and maintenance of natural IELs<sup>55</sup>. Indeed, we discovered that IL-15 levels were lower in the small intestines of mice given either the purified diet or the MS DKO mice. Consistently, the restoration of IL-15 levels to those in wild-type SPF mice rescued the reduced number of natural IELs. Thus, our findings show that dietary nucleic acids activate the MAVS and STING sensing pathways to induce IL-15 expression for natural IELs maintenance in the small intestine. In addition, we also observed a slight reduction in the number of natural IELs in *Myd88*-deficient mice, which is consistent with earlier research<sup>21</sup>. However, we found that STING and MAVS sensing pathways had a greater impact than MyD88 signaling on the maintenance of the natural IELs. Although the microbiota-driven MyD88 pathway is widely assumed to promote the maintenance of natural IELs<sup>21</sup>, our results in GF mice support previous reports that microbiota is dispensable for the maintenance of the natural IELs<sup>17,18</sup>. Thus, our data suggest that dietary nucleic acids, instead of microbiota, trigger innate sensing pathways, including MAVS, STING, and maybe MyD88, to maintain natural IELs in the small intestine.

While the functional mechanisms of the natural IELs are still not clear<sup>11</sup>, these IELs show a gene expression profile for a regulatory role<sup>40</sup>. Consistently, the natural IELs play essential roles in the suppression of colitis<sup>56,57</sup> and in the induction of oral tolerance<sup>34–37</sup>. Similarly, we found that the adoptive transfer of the natural IELs restored defective OVA-induced oral tolerance in the purified diet-fed mice or the MS DKO mice, suggesting that dietary nucleic acids activate the MAVS and STING pathways to maintain the natural IELs for oral tolerance. Treg cells have been demonstrated to play a central role in oral tolerance<sup>7,44</sup>. We found that the induction of antigen-specific Treg cells was impaired in both MS DKO mice and the purified diet-fed mice. We further demonstrated that adoptive transfer of the natural IELs restored the impaired OVA-induced antigen-specific Treg cells in the purified diet-fed mice or the MS DKO mice, indicating that the natural IELs can promote Treg cell development for oral tolerance. However, it remains unclear how the natural IELs promote Treg cell development. It has been revealed that small intestinal LP CD103<sup>+</sup> DCs can migrate to mesenteric lymph nodes to induce antigen-specific Treg cells<sup>45,46</sup>. Integrin  $\alpha\beta 8$ , a specific cell surface integrin expressed in the CD103<sup>+</sup> DCs, is required for the activation of TGF- $\beta 1$  from its inactive or latent precursor for the DCs to function<sup>48–50</sup>. *Itgb8*, which encodes  $\beta 8$ , is specifically expressed in the CD103<sup>+</sup> DCs, and is attained in the small intestine<sup>42</sup>. However, it is unclear how particular microenvironmental signals and cell lineages interact to activate the CD103<sup>+</sup> DCs for Treg cell induction. Here, we found that the natural IELs in the small intestine promoted  $\beta 8$  expression in CD103<sup>+</sup> DCs by producing TGF- $\beta 1$  in the OVA-induced oral tolerance model. Taken together, our data suggest that dietary nucleic acid-mediated innate sensing pathways maintain natural IELs, and the IELs, in turn, produce TGF- $\beta 1$  to promote

the function of tolerogenic CD103<sup>+</sup> DCs for Treg cell development and oral tolerance.

Then what is the relevance of the diets employed in our animal research to the human situation? So far, there are no reports showing direct evidence linking natural IEL defects to dietary tolerance in humans, due in part to the difficulties of obtaining and evaluating human samples. Nonetheless, a prior meta-analysis included 9 randomized controlled trials that examined the effects of nucleotide-supplemented formula milk on the immune response. Supplemented formula milk was significantly associated with a better antibody response to immunization and fewer occurrences of diarrhea than formula without nucleotides<sup>58</sup>. While we demonstrate here that dietary nucleic acids play an important role in oral tolerance by maintaining natural IELs, other food-derived substances, such as vitamin A, which can be converted to retinoic acids to promote Treg cell development, are also important for oral tolerance as well<sup>59–61</sup>. In addition, the gut microbiota can also promote the development and maintenance of Treg cells to maintain oral tolerance and intestinal quiescence<sup>62</sup>. Thus, the intestine has developed multiple immune tolerance systems to cope with both food- and microbiota-derived challenges to maintain gut homeostasis. To support this, a recent report has shown that small intestine LP  $\gamma\delta^+$  T cells could also contribute to oral tolerance by selecting tolerogenic microbes<sup>63</sup>. Considering the difference in the development, maintenance, and function of  $\gamma\delta$  T cells from different locations<sup>64</sup>, we speculated that the  $\gamma\delta$  T cells in distinct mucus compartments may respond differentially to dietary nutrients or microbiota. Thus, we hypothesized that intraepithelial or LP  $\gamma\delta$  T may cooperate to regulate oral tolerance in response to dietary nucleic acids or luminal microbiota. Additionally, as previous studies have shown that natural IELs have an immunoregulatory gene profile<sup>8,40</sup>, they may play a role in regulating intestinal homeostasis, maintaining epithelial barrier integrity, responding swiftly to infections, and initiating as well as modulating both adaptive and innate immune responses. The reduction of nucleic acid-induced natural IELs may also limit the protective function of IELs and increase susceptibility to disease, which requires further investigation.

In conclusion, we demonstrate that dietary nucleic acids, rather than microbiota, promote the development and maintenance of natural IELs through innate sensing pathways, and that natural IELs, in turn, contribute to the establishment of oral tolerance to protein antigen challenge.

## Methods

### Mice

C57BL/6 (Strain #000664), *Tnfr $\alpha$* <sup>−/−</sup> (Strain #005540), *Mavs*<sup>−/−</sup> (Strain #008634), *Sting*<sup>gt/gt</sup> (Strain #017537), *Rag1*<sup>−/−</sup> (Strain #002216), *Trif*<sup>−/−</sup> (Strain #005037) and OT-II (Strain #004194) mice were from Jackson Laboratory. *Mavs*<sup>−/−</sup> mice were first backcrossed into C57BL/6 background for at least four generations and then intercrossed with *Sting*<sup>gt/gt</sup> mice to obtain *Mavs*<sup>−/−</sup> *Sting*<sup>gt/gt</sup> double knockout mice. *Myd88*<sup>−/−</sup> mice were obtained from the Model Animal Research Center of Nanjing University (Nanjing, China)<sup>65</sup>. *Tbk*<sup>+/−</sup> (NM-KO-215091) mice were generated by CRISPR-Cas9 from Shanghai Model Organisms Center, Inc (Shanghai, China). Then *Tnfr $\alpha$* <sup>−/−</sup> mice were intercrossed with *Tbk*<sup>+/−</sup> mice to obtain *Tnfr $\alpha$* <sup>−/−</sup> *Tbk*<sup>+/−</sup> double knockout mice. *Ifnar*<sup>−/−</sup> mice were obtained from WT mice intercrossed with *Ifnar1*<sup>−/−</sup> *Ifngr1*<sup>−/−</sup> double knockout mice, which were kindly provided by Dr. Qibin Leng (Guangzhou Medical University, Guangzhou, China). *Ifnb1*<sup>−/−</sup> (S-KO-02581) mice and *Il15*<sup>+/−</sup> (S-KO-02624) mice were purchased from Cyagen Biosciences Inc. *Itgb7*<sup>−/−</sup> mice were kindly provided by Dr. Jianfeng Chen (Shanghai Institute of Biochemistry and Cell Biology, Chinese Academy of Sciences, Shanghai, China). C57BL/6 (CD45.1<sup>+</sup>) mice were kindly provided by Dr. Yichuan Xiao (Shanghai Institute of Nutrition and Health, Chinese Academy of Sciences, Shanghai, China). *Ahr*<sup>−/−</sup> and Cas9-KI mice were kindly provided by Dr. Ju Qiu (Shanghai Institute of



Nutrition and Health, Chinese Academy of Sciences, Shanghai, China). CD45.1<sup>+</sup> OT-II mice were obtained from OT-II mice intercrossed with CD45.1<sup>+</sup> C57BL/6 mice. All the above mice were housed in standard SPF facilities at the Shanghai Institute of Nutrition and Health (SINH), and littermates from each mouse line were bred as strict controls. GF C57BL/6 mice were maintained in GF isolators or purchased from Shanghai SLAC Laboratory Animal Co. (Shanghai, China) or Gem-Pharmatech Co., Ltd. (Nanjing, China). All animals were maintained under a 12 hr-12 hr light-dark cycle and received gamma-irradiated (50 kGy) pellet chow. A temperature of 20–24 °C and a humidity of 40–60% were used as housing conditions. All genetically modified mice and their control mice in the C57BL/6 background were subjected to experiments at the ages of 6–12 weeks. Both male and female mice were used in this study. For dietary treatment experiments, 3-week-old C57BL/6 wild-type mice or genetically deficient mice were fed either a sterilized normal diet (P1103F, Shanghai SLAC Laboratory Animal Co., Ltd, China) or a purified diet (AIN-93G, TD94045, ENGIVO or AIN-93M, Trophic Animal Feed High-Tech Co., Ltd, China) for 6–8 weeks. For the dietary nucleic acids supplementation, 0.25% purified salmon testes DNA (G8670, Solarbio LIFE SCIENCES, China) and 0.25% purified yeast RNA (D8030, Solarbio LIFE SCIENCES, China) were added to the purified diet. All animal studies were conducted under the Guide for the Care and Use of Laboratory Animals and were approved by the Institutional Biomedical Research Ethics Committee of the Shanghai Institute of Nutrition and Health (SINH-2023-QYC-1).

### Reagents and cell lines

Rabbit polyclonal anti-GAPDH (AP0063, 1:2000) was from Bioworld. Mouse monoclonal anti-TGF- $\beta$ 1 (141402, 1:1000) were from Biolegend. Rabbit polyclonal anti-TGF- $\beta$ 3 (A8460, 1:1000) was from ABclonal. Mouse monoclonal anti-CAS9 (7A9-3A3, sc-517386, 1:1000) was from Santa Cruz Biotechnology. Rabbit polyclonal anti-ITGB8 (29775, 1:100) was from Proteintech. Lipofectamine 3000 reagents were from Invitrogen Life Technologies. Ampicillin (A610028), Vancomycin (A600983), Metronidazole (A600633), and Neomycin (NB0366) were from Sangon Biotech. Aciclovir (S1807), Ribavirin (S2504), and Lamivudine (S1706) were from Selleck. Polybrene (TR-1003) was from MERCK. Recombinant mouse IL-15 (S66302) and mouse IL-3 (S75502) were from Biolegend. Recombinant Mouse IL-2 (212-12-20), mouse IL-4 (AF-214-14-20), and mouse EGF (AF-315-09-1000) were from Peprotech. Recombinant mouse TGF- $\beta$ 1 (CY97) and TGF- $\beta$ 3 (CJ44) were from Novoprotein. Plat-E (kindly provided by Dr. Xing Chang, Westlake University) and HEK293A (kindly provided by Dr. Huangtian Yang, Shanghai Institute of Nutrition and Health) were maintained in Dulbecco's modified Eagle's medium (DMEM; HyClone) supplemented with 10% (v/v) heat-inactivated fetal bovine serum (FBS, Gibco) and 100 U/mL penicillin and streptomycin. All cell lines were routinely tested for mycoplasma contamination, and mycoplasma-free cells were utilized for the study.

### Cell preparation

Thymocytes and splenocyte suspensions were prepared by mashing the organs through 40- $\mu$ m cell strainers. For isolation of Peyer's patches (PPs) and mesenteric lymph node (MLN) cells, the organs were cut into small pieces, enzymatically digested with Collagenase IV (0.5 mg/mL, Sigma) at 37 °C for 15 min, and then filtered before analysis. For IELs and lamina propria lymphocytes (LPLs) isolation, the small intestine or colon was opened longitudinally and washed with PBS containing 0.1% BSA, 100 U/mL penicillin, and 100  $\mu$ g/mL streptomycin three times. After removing Peyer's patches, the specimen was cut into 1-cm-long pieces and then shaken with pre-warmed 1 $\times$  Hank's buffer containing 1 mM DTT, 5 mM EDTA, 100 U/mL of penicillin, 100  $\mu$ g/mL of streptomycin, and 2% FCS for 30 min at 250 rpm, 37 °C. Supernatants were then collected and filtered through 70- $\mu$ m cell strainers followed by separation on 40–80% Percoll density

gradient (GE Healthcare). The cells that layered between the 40–80% fractions were collected as IELs. For LPL isolation, tissues were shaken in 1 $\times$  Hank's buffer containing 1 mM DTT, 5 mM EDTA, and 5% FCS at 200 rpm, 37 °C for 15 min. This step was repeated, and the supernatants were discarded. Then the tissues were further digested in RPMI 1640 supplemented with 0.5 mg mL<sup>-1</sup> of collagenase VIII (Sigma), 0.1 mg mL<sup>-1</sup> DNase I (Sigma), and 10% FCS at a shaking speed of 200 rpm, 37 °C for 30 min. Released cells were then subjected to Percoll fractionation as described above for isolation of LPLs.

### Flow cytometry and cell sorting

Suspensions of lymphocytes were prepared by sieving and gentle pipetting. Then cells were washed with ice-cold FACS buffer (2% FCS and 2 mM EDTA in PBS) and subsequently stained with appropriate antibodies for 30 min. Antibodies for flow cytometry were purchased from Thermo Fisher Scientific or Biolegend as follows: CD45-FITC and -EFLUOR 450 (30-F11); CD45.1-FITC, -PerCP-Cyanine5.5 and -PE-Cy7 (A20); CD45.2-PE and -APC (104); TCR- $\gamma\delta$ -PE and -PE-Cy7 (GL3); TCR- $\beta$ -FITC and -PerCP-Cyanine5.5 (H57-597); CD8 $\alpha$ -FITC, -PE-Cy7 and -APC (53-6.7); CD8 $\beta$ -FITC, -PE and -APC (EBIOH35-17.2); CD4-PE, -PerCP-Cyanine5.5 and -APC (RM4-5); CD11b-PE and -APC (M1/70); CD11c-FITC, -PE, and -APC (N418); CD3e-FITC, -PE, -PE-Cy7 and -APC (145-2C11); NK1.1-FITC, -PE and -PE-Cy7 (PK136); CD19-FITC and -PE-Cy7 (H1B19); FOXP3-PE (FJK-16s); CD25-APC (PC61.5); CD62L-PE-Cy7 (MEL-14); EpCAM-PerCP-Cyanine5.5, -APC (G8.8); CD64-PerCP-Cyanine5.5 (X54-5/7.1); MHC-II-PE-Cy7 (M5/114.15.2); CD103-APC and -BV421 (2E7); Bcl6-APC (7D1); GL7-FITC (GL7); CD38-FITC (90); PE-conjugated donkey anti-rabbit IgG antibody (Poly4064). Mouse AHR APC-conjugated Antibody (IC6697A) was from R&D. For cell surface staining, antibodies were diluted as 1:200. For intracellular staining, antibodies were diluted as 1:100. After washing twice with FACS buffer, the stained cells were subjected to analysis by the Beckman Gallios flow cytometer or sorted by Beckman MoFlo Astrios. Intracellular staining was performed according to the protocol of the Foxp3/Transcription Factor Staining Buffer set (eBiosciences). FlowJo\_V10 software was used for data analysis. For natural IELs transfer, the IELs were first enriched by CD8 $\alpha$  microbeads after separation on a discontinuous Percoll gradient, then followed by flow sorting for much higher purity IELs (EpCAM<sup>+</sup> DAPI<sup>+</sup> CD45<sup>+</sup> CD3<sup>+</sup> CD8 $\alpha$ <sup>+</sup> CD8 $\beta$ <sup>+</sup> CD4<sup>+</sup>), which reached 98%.

### Measurement of nucleic acids

For analysis of the amount of nucleic acids in the diet, a fresh pelleted diet from a normal diet or purified diet was ground to the dust in the liquid nitrogen. An appropriate amount of the diet dust was then weighed and subjected to nucleic acid extraction with a DNA extraction kit and RNA extraction kit. For analysis of the amount of nucleic acids in the mucus, duodenums were isolated and opened longitudinally and food debris was removed carefully. The mucus was harvested with PBS containing 0.5 mM dithiothreitol (PBS-DTT) and incubated for 3 min with gentle shaking. It was then centrifuged for 10 min at 11,000  $\times g$  to harvest released nucleic acids. This step was repeated twice and the supernatant was pooled, followed by nucleic acid extraction with a DNA extraction kit and RNA extraction kit. The concentration and quality of extracted DNA or RNA were determined by NanoDrop 2000.

### Serum biochemistry

Serum was collected from 8-week-old mice fed purified or normal diet since weaning after 2 h of fasting. Serum analysis was performed by Hitachi 7080 Chemistry Analyzer using standard protocols.

### Fluorescence in situ hybridization (FISH) and immunofluorescence

For the FISH experiment, unwashed duodenum tissues were fixated in Carnoy's fixative composed of 60% methanol, 30% chloroform, and

10% acetic acid, followed by embedding in paraffin. 8- $\mu$ m sections were cut, de-waxed, and hydrated. Then sections were blocked with 1% BSA in PBS and hybridized to a FITC-conjugated pan-bacteria probe directed against the 16S rRNA gene: EUB338 (5'-GCTGCCTCCCGTAG-GAGT-3') at 10 nM in 200  $\mu$ L of hybridization buffer (50 mM NaCl, 100 mM Tris-HCl (pH 7.4), 5 mM EDTA, 10% dextran sulfate) at 40 °C for 16 h. Sections were rinsed in wash buffer (50 mM NaCl, 4 mM Tris-HCl (pH 7.4), and 0.02 mM EDTA) at 45 °C for 20 min and then counterstained with DAPI. For the tracking of fluorescence-labeled nucleic acids, the mice were administered with 40  $\mu$ g synthesized Cy-5-conjugated dsDNA re-suspended in 200  $\mu$ L PBS by oral gavage. After 1 hour, the mice were euthanized (by cervical dislocation) to collect unwashed duodenum tissues, followed by fixation in above Carnoy's fixative. Frozen sections were washed and stained with DAPI. Tissues were visualized using a fluorescence microscope (Zeiss Axio Imager A2).

### Cell proliferation and apoptosis analysis

For the cell proliferation analysis, IELs isolated from the small intestine of the indicated mice were stained with the appropriate antibodies, then fixed and permeabilized by the Perm&Fix kit, and subsequently incubated with anti-Ki67-PE-Cy7 (Sola15) for 30 min. After washing, cells were analyzed on the Beckman Gallios flow cytometer. For analysis of apoptosis, cells were stained with an Annexin-V staining kit according to the manufacturer's protocol.

### Adenovirus-mediated gene expression in mice

Briefly, the sequence encoding mouse IL-15 was cloned into the pAdTrack-CMV vector and then recombined with the pAdEasy-1 vector. Recombinant Adv-IL-15 or empty vector (Adv-EV) was transfected into HEK293A cells. After virus package, amplification, and titration,  $2 \times 10^9$  adenovirus particles in 200  $\mu$ L PBS were intravenously injected into the indicated mice under different experimental settings. After 2 weeks, the mice were either euthanized for the analysis or used for in vivo experiments.

### Real-time PCR

RNAs were extracted from cells or tissues by Trizol reagent (Invitrogen) according to the manufacturer's instructions and then reverse transcribed into cDNA by One-Step PrimeScript RT-PCR Kit (Takara). The cDNAs were used for real-time PCR analysis with the indicated primer sets and SYBR Green PCR Master Mix (Takara). The PCR was run by the Step One Plus Real-Time PCR systems (VIA7, Applied Biosystems). Real-time PCR primers (Sangon) used for murine *Rpl13a*, *Il15*, *Il7*, *Il10*, *Tgfb1*, *Tgfb2*, *Tgfb3*, *Itgav*, *Itgb6*, and *Itgb8* are listed in the Supplementary Table 1. The PCR conditions were 95 °C for 1 min, followed by 40 cycles with denaturation at 95 °C for 5 s and annealing and extension at 60 °C for 30 s.

### Immunoblot analysis

Briefly, the cells were harvested after the indicated stimulation, washed with ice-cold PBS two times, and then lysed with the lysis buffer containing 50 mM HEPES pH 7.4, 150 mM NaCl, 5 mM EDTA, 10% glycerol, 1% Nonidet P-40 in deionized water (ddH<sub>2</sub>O) and protease inhibitors. Lysates were centrifuged at 13,000  $\times g$  at 4 °C for 15 min. Protein concentration was determined by the Bradford method. During the pre-run, the supernatant was boiled with 2 $\times$  PAGE loading buffer 1:1 (v/v) containing 125 mM Tris-HCl pH 6.8, 30% glycerol, and 0.1% bromophenol blue in ddH<sub>2</sub>O for 10 minutes, and then followed by PAGE analysis.

### ELISA

Cell supernatants from the indicated cell cultures or the lysates of homogenized intestinal tissues were collected and then assayed for mouse IL-15 (R&D Systems), IFN- $\gamma$  (R&D Systems), IL-2 (Biolegend),

TGF- $\beta$ 1 (Invitrogen) and TGF- $\beta$ 3 (Boster) according to the manufacturer's instructions.

### Cohousing, commensal virus and bacteria depletion, and microbiota reconstitution

For cohousing experiments, ~4-week-old age and sex-matched mice were transferred into an isolator cage in the same room and on the same diet for at least 4 weeks. For microbiota reconstitution experiments, intestinal microbiota was depleted by an antibiotic cocktail of 1 g/L each of Ampicillin, Neomycin sulfate, Metronidazole, and 0.5 g/L Vancomycin hydrochloride in drinking water weekly. The antibiotic activity was gauged by changes in cecum size due to bacterial death, as well as fecal bacterial 16S rDNA measurement by stool DNA extraction kit. After 4 weeks, the antibiotics-treated mice were randomly separated, transferred into new isolator cages, and gavaged with 200  $\mu$ L of fecal bacteria obtained by homogenizing the full contents of feces from the corresponding donor mice in 50 ml water. For commensal virus depletion, an AVC was utilized. Briefly, 3-week-old mice were orally given an AVC containing ribavirin (30 mg/kg), lamivudine (10 mg/kg), and aciclovir (20 mg/kg) once a day for 5 weeks.

### 16S ribosomal DNA gene sequencing

Microbial DNA was extracted from the fecal samples of the indicated mice by using the QIAamp Fast DNA Stool Mini Kit (QIAGEN) according to the manufacturer's protocols. The quality and concentration of DNA were determined by 1.0% agarose gel electrophoresis and a NanoDrop® ND-2000 spectrophotometer (Thermo Scientific Inc.). The V3-V4 regions of the bacteria 16S ribosomal RNA gene were amplified by an ABI GeneAmp® 9700 PCR thermocycler (ABI) with the following primers: 338 F 5'-barcode-CTCTACGGAGGCAGCA-3' and 806 R 5'-GGACTACHVGGGTWTCTAAT-3' (the barcode is an 8-base sequence unique to each sample). The PCR product was extracted from 2% agarose gel and purified using the AxyPrep DNA Gel Extraction Kit (Axygen Biosciences) according to the manufacturer's instructions and quantified using Quantus™ Fluorometer (Promega). Purified amplicons were pooled in equimolar amounts, and paired-end sequenced on an Illumina MiSeq PE300 platform/NovaSeq PE250 platform (Illumina) according to the standard protocols by Majorbio Bio-Pharm Technology Co. Ltd. (Shanghai, China). After demultiplexing, the resulting sequences were quality-filtered with fastp (0.19.6) and merged with FLASH (v1.2.11). Then the high-quality sequences were de-noised using the DADA2 plugin in the Qiime2 (version 2020.2) pipeline with recommended parameters, which obtains single nucleotide resolution based on error profiles within samples. DADA2-de-noised sequences are usually called amplicon sequence variants (ASVs). Taxonomic assignment of ASVs was performed using the Naive Bayes consensus taxonomy classifier implemented in Qiime2 and the SILVA 16S rRNA database (v138). The data were analyzed on the online platform of Majorbio Cloud Platform (<https://www.majorbio.com/>).

### Bacterial genomic DNA isolation and microbiota analysis

For the fecal transplant experiments, fecal samples were collected and processed for DNA isolation using the QIAamp Fast DNA Stool Mini Kit (QIAGEN). To determine the relative abundance of different intestinal bacterial groups, isolated bacterial genomic DNA was amplified for 16S rDNA with a One-Step PrimeScript RT-PCR Kit (Takara). Specific 16S rDNA primer sequences for real-time PCR are listed in Supplementary Table S1.

### Adoptive transfer

For the oral tolerance model,  $1 \times 10^6$  pooled small intestinal total natural IELs (DAPI<sup>+</sup> EpCAM<sup>+</sup> CD45<sup>+</sup> CD3<sup>+</sup> CD8 $\alpha$ <sup>+</sup> CD8 $\beta$ <sup>+</sup> CD4<sup>-</sup>) or  $5 \times 10^5$  TCR $\gamma$  $\delta$ <sup>+</sup> IELs (DAPI<sup>+</sup> EpCAM<sup>+</sup> CD45<sup>+</sup> CD3<sup>+</sup> TCR $\gamma$  $\delta$ <sup>+</sup> CD8 $\beta$ <sup>+</sup> CD4<sup>-</sup>) or TCR $\alpha$  $\beta$ <sup>+</sup> CD8 $\alpha$ <sup>+</sup> IELs (DAPI<sup>+</sup> EpCAM<sup>+</sup> CD45<sup>+</sup> TCR $\beta$ <sup>+</sup> CD8 $\alpha$ <sup>+</sup> CD8 $\beta$ <sup>+</sup> CD4<sup>-</sup>) were isolated from 10-week-old WT mice by flow cell sorting, and then i.v. transferred into the

indicated recipient mice. 2 weeks later, the mice were subjected to the analysis of the oral tolerance model. For BM chimera experiments,  $5 \times 10^6$  BM cells from 8-week-old WT or *Mavs*<sup>-/-</sup>*Sting*<sup>tg/tg</sup> mice were intravenously transferred into *Rag1*<sup>-/-</sup> mice,  $5 \times 10^6$  WT or *Mavs*<sup>-/-</sup>*Sting*<sup>tg/tg</sup> BM cells were intravenously transferred into lethally irradiated WT or *Mavs*<sup>-/-</sup>*Sting*<sup>tg/tg</sup> mice, or  $5 \times 10^6$  WT or *Il15*<sup>-/-</sup> BM cells were intravenously transferred into lethally irradiated WT or *Il15*<sup>-/-</sup> mice. 8 weeks after BM transfer, the chimera mice were euthanized to analyze IELs by flow cytometry.

### Oral tolerance

For OVA-induced oral tolerance, mice were fed daily 5 mg ovalbumin (OVA, Sigma, and Grade V) via oral gavage for 5 days. Control mice were given PBS alone. One week after the last feeding, all mice were immunized subcutaneously with 100 µg OVA protein emulsified in 100 µL CFA (Sigma). For detection of the levels of OVA-specific antibodies in serum, those mice were euthanized to collect serum 10 days after s.c. immunization. Meanwhile, spleen cells were collected and stimulated in 96-well plates as triplicates with 100 µg/mL OVA protein. The supernatant effector cytokines (IFN-γ and IL-2) were then measured by ELISA after 3 days of treatment. To establish systemic unresponsiveness to a high dose of oral antigen, mice were given 25 mg of OVA dissolved in 0.25 mL of PBS by gastric intubation. Control mice received PBS only. Seven days later, mice were immunized s.c. with 100 µg of OVA in 100 µL of complete Freund's adjuvant (OVA/CFA). For the OVA/cholera toxin allergy model, mice were given drinking water with 0.1% OVA for three days. One week later, 1 mg OVA + 20 µg cholera toxin (100B; List Biological) in 0.2 M sodium bicarbonate was administered once per week for three weeks, with endpoint examination two days following the final dosage. 1 day before the endpoint, serum was collected for ELISA. For anaphylaxis experiments, OVA or OVA/CT was given once a week for four weeks, followed by a challenge seven days following the final dosage. Mice were given 5 mg OVA i.p., and their body temperatures were measured every 10 minutes for 50 minutes using digital thermometers.

### Delayed-type hypersensitivity

For delayed-type hypersensitivity (DTH) detection, one week after the last feeding of OVA, mice were injected subcutaneously with 200 µL OVA/CFA emulsion (250 µg OVA plus 100 µL CFA, Sigma) in the tail base. Seven days later, the mice were challenged with 50 µL of aggregated OVA (10 µg/mL) injected into the left footpad while the right footpad (control) received 50 µL of phosphate-buffered saline (PBS). After 24 hours, the thickness of both hind footpads was measured with a caliper. Specific DTH was calculated as the difference between the left and the right footpad.

### Serum OVA-specific immunoglobulin levels

OVA-specific IgE, IgG1, and IgG2a were measured by enzyme-linked immunosorbent assay. Anti-OVA IgE (2C6, Invitrogen), Anti-OVA IgG1 (L71, Biozol), and Anti-OVA IgG2a (M12E4D5, Chondrex) were used as standards. Rat anti-mouse IgE-HRP (23G3, SouthernBiotech), Goat anti-mouse IgG1-HRP (X56, BD Pharmingen), Rat Anti-Mouse IgG2a-HRP (SB84a, SouthernBiotech) and were used for detection. The serum samples were diluted with BSA/PBS at 1/500 for IgG1 and IgG2a measurements and 1/10 for IgE measurements to obtain an optical density (OD) reading on a linear curve from the serial dilutions.

### Retroviral infection and adoptive transfer of IELs

For generating the indicated knockout IELs by the CRISPR-Cas9 approach, the protocol was adapted from the previous reports<sup>66,67</sup>. Primarily, the gRNA targeting sequences for the indicated genes were cloned into the Retro-sgRNA-eGFP vector. The target sequences used for *Tgfb1*, and *Tgfb3* are CAACAGCACCCGCGACCGGG and GAT

GTGGCCGAAGTCCAACG separately. Then, retrovirus was produced by transfecting Plat-E cells with the above plasmids, and the supernatant containing fresh virus was collected and used to infect Cas9 IELs. Small intestinal Cas9 IELs were isolated as above described and re-suspended with cRPMI (RPMI 1640, 10% FCS, 100 U/mL penicillin 100 µg/mL streptomycin, 2 mM glutamine, 1 mM sodium pyruvate, 1 mM β-mercaptoethanol, 2.5 mM HEPES, and non-essential amino acids) to a final concentration of  $1 \times 10^6$  cells/mL. To infect Cas9 IELs, Cas9 IELs were first stimulated on plate-bound anti-CD3 antibody (1 µg/mL) in a cocktail of cytokines (IL-2 (10 ng/mL), IL-15 (100 ng/mL), IL-3 (20 ng/mL), and IL-4 (20 ng/mL)) for 24 h. The activated T cells were spin-infected for 1.5 hours at 2000 rpm in the presence of polybrene (8 µg/mL) twice at 18 hours and 36 hours post-activation, followed by being transferred to fresh plates and incubated with IL-2 (10 ng/mL) in cRPMI at 37 °C for 3 days. On day 3 of culture, GFP-positive natural IELs were sorted and collected, washed with ice-cold PBS, and re-suspended to a final concentration of  $5 \times 10^6$  cells/mL.  $1 \times 10^6$  cells were injected intravenously into each mouse.

### Bulk RNA-seq

Small intestine LP CD103<sup>+</sup> DCs of WT mice at steady condition or after oral gavage of 5 mg OVA for 3 days were flow sorted and pooled ( $1 \times 10^5$ ). Total RNA was extracted by RNA extraction kit (Tiangen Biotech). RNA quality was examined with an Agilent Bioanalyzer 2100 (Agilent), and samples with the RNA integrity (RIN) number >8 were submitted to the TIANGEN Biotech for library preparation and sequencing (Illumina HiSeq PE150). The generated raw data (raw reads) of fastq format were first processed through in-house Perl scripts. Clean data (clean reads) were obtained by removing reads containing adapter and trimming low-quality base with Trimmomatic. Mm10 mouse reference genome and gene model annotation files were downloaded from the genome website directly. An index of the reference genome was built and paired-end clean reads were aligned to the reference genome using Hisat2 v2.0.5. Htseq-count was used to count the read numbers mapped to each gene. Then FPKM of each gene was calculated based on the length of the gene and the read count mapped to this gene. Differential expression analysis of two conditions/groups (two biological replicates per condition) was performed using the DESeq2 R package (1.16.1). The resulting *P* values were adjusted using Benjamini and Hochberg's approach for controlling the false discovery rate. Visualization of differential gene expression with volcano plot was created on the online platform Sangerbox (<http://www.sangerbox.com/>).

### Adoptive transfer and antigen-specific Treg cell assessment

Spleens and peripheral lymph nodes were removed from CD45.1<sup>+</sup> OT-II mice. Naïve CD45.1<sup>+</sup>CD3<sup>+</sup>CD25<sup>-</sup>CD8α<sup>-</sup>CD4<sup>+</sup>CD62L<sup>+</sup> T cells were isolated by flow cell sorting. Then  $1 \times 10^6$  sorted cells were intravenously transferred into the indicated recipient mice. One day later, mice were provided with 5 mg/mL OVA ad libitum in drinking water; control subjects received normal drinking water. After 7 days, the lymphocytes of mesenteric lymph nodes (MLNs) and small intestinal LP were harvested. CD45.1<sup>+</sup>CD4<sup>+</sup> Foxp3<sup>+</sup> Treg cell counts as a percentage of total CD45.1<sup>+</sup>CD4<sup>+</sup> T cells were determined by flow cytometry.

### In vitro Treg differentiation

Naïve CD45.1<sup>+</sup>CD3<sup>+</sup>CD8α<sup>-</sup>CD4<sup>+</sup>CD62L<sup>+</sup>CD25<sup>-</sup> OT-II Tg CD4<sup>+</sup> T cells ( $8 \times 10^4$ ) and small intestine lamina LP CD103<sup>+</sup> DCs ( $2 \times 10^4$ ) from the indicated oral OVA pre-treated mice were flow sorted, followed by co-culture in medium cRPMI (RPMI 1640, 10% FCS, 100 U/mL penicillin 100 µg/mL streptomycin, 2 mM glutamine, 1 mM sodium pyruvate, 1 mM β-mercaptoethanol, 2.5 mM HEPES, and non-essential amino acids) for 3 days. Following the removal of DCs using anti-CD11c



microbeads (Miltenyi Biotec), flow cytometry was used to examine CD4<sup>+</sup> cells expressing Foxp3.

### Statistical analysis

Data are presented as the mean  $\pm$  SEM. Differences between groups were evaluated by analysis of variance followed by a Bonferroni post hoc test or by a two-tailed Student's *t* test with 95% confidence intervals. *p* values < 0.05 were considered statistically significant. GraphPad Prism 8.0 software was used for statistical analysis.

### Reporting summary

Further information on research design is available in the Nature Portfolio Reporting Summary linked to this article.

### Data availability

16S rRNA sequencing and bulk RNA-seq data have been deposited in the NCBI Sequence Read Archive (SRA) under accession number SRA: PRJNA906202 (<https://www.ncbi.nlm.nih.gov/sra/?term=PRJNA906202>) and SRA: PRJNA906645 (<https://www.ncbi.nlm.nih.gov/sra/?term=PRJNA906645>) respectively. The remaining data are available within the Article, Supplementary Information or Source Data file. Source data are provided with this paper.

### Code availability

No custom code was created for this paper.

### References

- Hooper, L. V., Littman, D. R. & Macpherson, A. J. Interactions between the microbiota and the immune system. *Science* **336**, 1268–1273 (2012).
- Garrett, W. S., Gordon, J. I. & Glimcher, L. H. Homeostasis and inflammation in the intestine. *Cell* **140**, 859–870 (2010).
- Jain, N. & Walker, W. A. Diet and host-microbial crosstalk in post-natal intestinal immune homeostasis. *Nat. Rev. Gastroenterol. Hepatol.* **12**, 14–25 (2015).
- Mowat, A. M. Anatomical basis of tolerance and immunity to intestinal antigens. *Nat. Rev. Immunol.* **3**, 331–341 (2003).
- Rezende, R. M. & Weiner, H. L. History and mechanisms of oral tolerance. *Semin Immunol.* **30**, 3–11 (2017).
- Tordesillas, L. & Berin, M. C. Mechanisms of oral tolerance. *Clin. Rev. Allergy Immunol.* **55**, 107–117 (2018).
- Pabst, O. & Mowat, A. M. Oral tolerance to food protein. *Mucosal Immunol.* **5**, 232–239 (2012).
- Cheroutre, H., Lambolez, F. & Mucida, D. The light and dark sides of intestinal intraepithelial lymphocytes. *Nat. Rev. Immunol.* **11**, 445–456 (2011).
- Van Kaer, L. & Olivares-Villagomez, D. Development, homeostasis, and functions of intestinal intraepithelial lymphocytes. *J. Immunol.* **200**, 2235–2244 (2018).
- Hoytema van Konijnenburg, D. P. & Mucida, D. Intraepithelial lymphocytes. *Curr. Biol.* **27**, R737–R739 (2017).
- Olivares-Villagomez, D. & Van Kaer, L. Intestinal intraepithelial lymphocytes: sentinels of the mucosal barrier. *Trends Immunol.* **39**, 264–275 (2018).
- McDonald, B. D., Jabri, B. & Bendelac, A. Diverse developmental pathways of intestinal intraepithelial lymphocytes. *Nat. Rev. Immunol.* **18**, 514–525 (2018).
- Ruscher, R. & Hogquist, K. A. Development, ontogeny, and maintenance of TCR $\alpha$ ph $\beta$ (+) CD8 $\alpha$ ph $\alpha$  IEL. *Curr. Opin. Immunol.* **58**, 83–88 (2019).
- Qiu, Y., Peng, K., Liu, M., Xiao, W. & Yang, H. CD8 $\alpha$ ph $\alpha$  TCR $\alpha$ ph $\beta$  intraepithelial lymphocytes in the mouse gut. *Dig. Dis. Sci.* **61**, 1451–1460 (2016).
- Chung, H. et al. Gut immune maturation depends on colonization with a host-specific microbiota. *Cell* **149**, 1578–1593 (2012).
- Bandeira, A. et al. Localization of gamma/delta T cells to the intestinal epithelium is independent of normal microbial colonization. *J. Exp. Med.* **172**, 239–244 (1990).
- Klose, C. S. et al. The transcription factor T-bet is induced by IL-15 and thymic agonist selection and controls CD8 $\alpha$ ph $\alpha$ (+) intraepithelial lymphocyte development. *Immunity* **41**, 230–243 (2014).
- Hoytema van Konijnenburg, D. P. et al. Intestinal epithelial and intraepithelial T cell crosstalk mediates a dynamic response to infection. *Cell* **171**, 783–794.e713 (2017).
- Kunisawa, J., Takahashi, I. & Kiyono, H. Intraepithelial lymphocytes: their shared and divergent immunological behaviors in the small and large intestine. *Immunol. Rev.* **215**, 136–153 (2007).
- Beagley, K. W. et al. Differences in intraepithelial lymphocyte T cell subsets isolated from murine small versus large intestine. *J. Immunol.* **154**, 5611–5619 (1995).
- Yu, Q. et al. MyD88-dependent signaling for IL-15 production plays an important role in maintenance of CD8  $\alpha$ ph $\alpha$  TCR  $\alpha$ ph $\beta$  and TCR gamma delta intestinal intraepithelial lymphocytes. *J. Immunol.* **176**, 6180–6185 (2006).
- Umesaki, Y., Setoyama, H., Matsumoto, S. & Okada, Y. Expansion of alpha beta T-cell receptor-bearing intestinal intraepithelial lymphocytes after microbial colonization in germ-free mice and its independence from thymus. *Immunology* **79**, 32–37 (1993).
- Li, Y. et al. Exogenous stimuli maintain intraepithelial lymphocytes via aryl hydrocarbon receptor activation. *Cell* **147**, 629–640 (2011).
- Liu, L. et al. Commensal viruses maintain intestinal intraepithelial lymphocytes via noncanonical RIG-I signaling. *Nat. Immunol.* **20**, 1681–1691 (2019).
- Ma, L. J., Acero, L. F., Zal, T. & Schluns, K. S. Trans-presentation of IL-15 by intestinal epithelial cells drives development of CD8 $\alpha$ ph $\alpha$  IELs. *J. Immunol.* **183**, 1044–1054 (2009).
- Schluns, K. S. et al. Distinct cell types control lymphoid subset development by means of IL-15 and IL-15 receptor alpha expression. *Proc. Natl. Acad. Sci. USA* **101**, 5616–5621 (2004).
- Marchlik, E. et al. Mice lacking Tbk1 activity exhibit immune cell infiltrates in multiple tissues and increased susceptibility to LPS-induced lethality. *J. Leukoc. Biol.* **88**, 1171–1180 (2010).
- Colpitts, S. L. et al. Cutting edge: the role of IFN- $\alpha$  receptor and MyD88 signaling in induction of IL-15 expression in vivo. *J. Immunol.* **188**, 2483–2487 (2012).
- Iurescia, S., Fioretti, D. & Rinaldi, M. Targeting cytosolic nucleic acid-sensing pathways for cancer immunotherapies. *Front. Immunol.* **9**, 711 (2018).
- Koyama, S. et al. Innate immune control of nucleic acid-based vaccine immunogenicity. *Expert Rev. Vaccines* **8**, 1099–1107 (2009).
- Pinheiro-Rosa, N. et al. Oral tolerance as antigen-specific immunotherapy. *Immunother. Adv.* **1**, ltab017 (2021).
- Tan, J. et al. Dietary fiber and bacterial SCFA enhance oral tolerance and protect against food allergy through diverse cellular pathways. *Cell Rep.* **15**, 2809–2824 (2016).
- Stephen-Victor, E. & Chatila, T. A. Regulation of oral immune tolerance by the microbiome in food allergy. *Curr. Opin. Immunol.* **60**, 141–147 (2019).
- Mengel, J. et al. Anti-gamma delta T cell antibody blocks the induction and maintenance of oral tolerance to ovalbumin in mice. *Immunol. Lett.* **48**, 97–102 (1995).
- Ke, Y., Pearce, K., Lake, J. P., Ziegler, H. K. & Kapp, J. A. Gamma delta T lymphocytes regulate the induction and maintenance of oral tolerance. *J. Immunol.* **158**, 3610–3618 (1997).
- Fujihashi, K. et al. gammadelta T cells regulate mucosally induced tolerance in a dose-dependent fashion. *Int. Immunol.* **11**, 1907–1916 (1999).
- Locke, N. R., Stankovic, S., Funda, D. P. & Harrison, L. C. TCR gamma delta intraepithelial lymphocytes are required for self-tolerance. *J. Immunol.* **176**, 6553–6559 (2006).



38. Gorf, G., Rivera-Nieves, J. & Ley, K. Role of beta7 integrins in intestinal lymphocyte homing and retention. *Curr. Mol. Med.* **9**, 836–850 (2009).
39. Wang, Y. C. et al. Intestinal cell type-specific communication networks underlie homeostasis and response to Western diet. *J. Exp. Med.* **220**, e20221437 (2023).
40. Denning, T. L. et al. Mouse TCRalpha $\beta$ +CD8alpha $\alpha$  intraepithelial lymphocytes express genes that down-regulate their antigen reactivity and suppress immune responses. *J. Immunol.* **178**, 4230–4239 (2007).
41. van Caam, A. et al. TGF $\beta$ -mediated expression of TGF $\beta$ -activating integrins in SSc monocytes: disturbed activation of latent TGF $\beta$ ? *Arthritis Res. Ther.* **22**, 42 (2020).
42. Boucard-Jourdin, M. et al. beta8 integrin expression and activation of TGF- $\beta$  by intestinal dendritic cells are determined by both tissue microenvironment and cell lineage. *J. Immunol.* **197**, 1968–1978 (2016).
43. Nishimura, S. L. Integrin-mediated transforming growth factor- $\beta$  activation, a potential therapeutic target in fibrogenic disorders. *Am. J. Pathol.* **175**, 1362–1370 (2009).
44. Wawrzyniak, M., O'Mahony, L. & Akdis, M. Role of regulatory cells in oral tolerance. *Allergy Asthma Immunol. Res.* **9**, 107–115 (2017).
45. Ruane, D. T. & Lavelle, E. C. The role of CD103(+) dendritic cells in the intestinal mucosal immune system. *Front. Immunol.* **2**, 25 (2011).
46. Scott, C. L., Aumeunier, A. M. & Mowat, A. M. Intestinal CD103+ dendritic cells: master regulators of tolerance? *Trends Immunol.* **32**, 412–419 (2011).
47. Siddiqui, K. R. & Powrie, F. CD103+ GALT DCs promote Foxp3+ regulatory T cells. *Mucosal Immunol.* **1**, S34–S38 (2008).
48. Paidassi, H. et al. Preferential expression of integrin  $\alpha$ v $\beta$ 8 promotes generation of regulatory T cells by mouse CD103+ dendritic cells. *Gastroenterology* **141**, 1813–1820 (2011).
49. Worthington, J. J., Czajkowska, B. I., Melton, A. C. & Travis, M. A. Intestinal dendritic cells specialize to activate transforming growth factor- $\beta$  and induce Foxp3+ regulatory T cells via integrin  $\alpha$ v $\beta$ 8. *Gastroenterology* **141**, 1802–1812 (2011).
50. Esebanmen, G. E. & Langridge, W. H. R. The role of TGF- $\beta$  signaling in dendritic cell tolerance. *Immunol. Res.* **65**, 987–994 (2017).
51. Ruemmele, F. M. & Garnier-Lengline, H. Transforming growth factor and intestinal inflammation: the role of nutrition. *Nestle Nutr. Inst. Workshop Ser.* **77**, 91–98 (2013).
52. Kim, K. S. et al. Dietary antigens limit mucosal immunity by inducing regulatory T cells in the small intestine. *Science* **351**, 858–863 (2016).
53. Nagafuchi, S. et al. Dietary nucleotides increase the proportion of a TCR  $\gamma$  $\delta$ + subset of intraepithelial lymphocytes (IEL) and IL-7 production by intestinal epithelial cells (IEC); implications for modification of cellular and molecular cross-talk between IEL and IEC by dietary nucleotides. *Biosci. Biotechnol. Biochem.* **64**, 1459–1465 (2000).
54. Tan, X., Sun, L., Chen, J. & Chen, Z. J. Detection of microbial infections through innate immune sensing of nucleic acids. *Annu. Rev. Microbiol.* **72**, 447–478 (2018).
55. Kennedy, M. K. et al. Reversible defects in natural killer and memory CD8 T cell lineages in interleukin 15-deficient mice. *J. Exp. Med.* **191**, 771–780 (2000).
56. Poussier, P., Ning, T., Banerjee, D. & Julius, M. A unique subset of self-specific intraintestinal T cells maintains gut integrity. *J. Exp. Med.* **195**, 1491–1497 (2002).
57. Inagaki-Ohara, K. et al. Mucosal T cells bearing TCR $\gamma$  $\delta$  play a protective role in intestinal inflammation. *J. Immunol.* **173**, 1390–1398 (2004).
58. Gutierrez-Castrellon, P. et al. Immune response to nucleotide-supplemented infant formulae: systematic review and meta-analysis. *Br. J. Nutr.* **98**, S64–S67 (2007).
59. Ye, J. et al. The aryl hydrocarbon receptor preferentially marks and promotes gut regulatory T cells. *Cell Rep.* **21**, 2277–2290 (2017).
60. Mucida, D. et al. Reciprocal TH17 and regulatory T cell differentiation mediated by retinoic acid. *Science* **317**, 256–260 (2007).
61. Prietl, B. et al. Vitamin D supplementation and regulatory T cells in apparently healthy subjects: vitamin D treatment for autoimmune diseases? *Isr. Med. Assoc. J.* **12**, 136–139 (2010).
62. Wu, R. Q., Zhang, D. F., Tu, E., Chen, Q. M. & Chen, W. The mucosal immune system in the oral cavity—an orchestra of T cell diversity. *Int. J. Oral. Sci.* **6**, 125–132 (2014).
63. Rezende, R. M. et al. Gamma-delta T cells modulate the microbiota and fecal micro-RNAs to maintain mucosal tolerance. *Microbiome* **11**, 32 (2023).
64. Rampoldi, F. & Prinz, I. Three layers of intestinal  $\gamma$  $\delta$  T cells talk different languages with the microbiota. *Front. Immunol.* **13**, 849954 (2022).
65. Adachi, O. et al. Targeted disruption of the MyD88 gene results in loss of IL-1- and IL-18-mediated function. *Immunity* **9**, 143–150 (1998).
66. Dong, M. B. et al. Systematic immunotherapy target discovery using genome-scale in vivo CRISPR screens in CD8 T cells. *Cell* **178**, 1189–1204 e1123 (2019).
67. Swamy, M. et al. Intestinal intraepithelial lymphocyte activation promotes innate antiviral resistance. *Nat. Commun.* **6**, 7090 (2015).

## Acknowledgements

This work was supported by grants from the National Key R&D Program of China (2020YFA0509100 and 2018YFA0507402), the National Natural Science Foundation of China (91842306, 81830018, and 32030039).

## Author contributions

Y.Q. and T.Y. designed the experiments and wrote the manuscript; T.Y. conducted the experiments and analyzed the data. T.L., Y.X., M.C., and M.Z. helped with the experiments. J.Q., Q.L., J.C., and G.H. provided reagents. X.S. helped edit the manuscript. Y.Q. supervised the study.

## Competing interests

The authors declare no competing interests.

## Additional information

**Supplementary information** The online version contains supplementary material available at

<https://doi.org/10.1038/s41467-024-53814-0>.

**Correspondence** and requests for materials should be addressed to Youcun Qian.

**Peer review information** *Nature Communications* thanks Mahima Swamy, Emmanuel Stephen Victor and the other, anonymous, reviewer(s) for their contribution to the peer review of this work. A peer review file is available.

**Reprints and permissions information** is available at

<http://www.nature.com/reprints>

**Publisher's note** Springer Nature remains neutral with regard to jurisdictional claims in published maps and institutional affiliations.

**Open Access** This article is licensed under a Creative Commons Attribution-NonCommercial-NoDerivatives 4.0 International License, which permits any non-commercial use, sharing, distribution and reproduction in any medium or format, as long as you give appropriate credit to the original author(s) and the source, provide a link to the Creative Commons licence, and indicate if you modified the licensed material. You do not have permission under this licence to share adapted material derived from this article or parts of it. The images or other third party material in this article are included in the article's Creative Commons licence, unless indicated otherwise in a credit line to the material. If material is not included in the article's Creative Commons licence and your intended use is not permitted by statutory regulation or exceeds the permitted use, you will need to obtain permission directly from the copyright holder. To view a copy of this licence, visit <http://creativecommons.org/licenses/by-nc-nd/4.0/>.

© The Author(s) 2024